Supplementary Information (SI) for Chemical Science.
This journal is © The Royal Society of Chemistry 2024

Single-Molecule Detection of a Terrylenediimide-Based Near-Infrared Emitter

Suvarna Sujilkumar, Philip Daniel Maret, Kavya Vinod, Athira T. John, and Mahesh Hariharan*

School of Chemistry, Indian Institute of Science Education and Research Thiruvananthapuram (IISER TVM), Maruthamala P. O., Vithura, Thiruvananthapuram 695551, Kerala, India.

*E-mail: mahesh@iisertvm.ac.in

Supporting Information (SI)

Table of Contents

Section 1: Materials and Methods

All chemicals were procured from commercial suppliers and utilized as received without further purification. Allreactions were carried out in oven-dried glassware prior to use. Solvents were dried and distilled by standard laboratory purification techniques. TLC analyses were performed on aluminum plates of silica gel 60 F254 plates (0.25 mm) from Merck and were visualized under short- and long-wavelength UV lamps. Column chromatography was performed using silica gel of 200-400 mesh employing a solvent polarity correlated with the TLC mobility observed for the substance of interest. Yields are reported for substances that are chromatographically and spectroscopically homogeneous. Melting points were determined using a capillary melting point apparatus. ^{1}H and ^{13}C NMR spectra were recorded on a 500 MHz Bruker advance DPX spectrometer, with tetramethylsilane (TMS) as the internal standard. High-resolution mass spectra (HRMS) were obtained using a Thermo scientific Q exactive mass spectrometer with Atmospheric pressure chemical ionization (APCI, positive mode). Photophysical measurements of the derivatives were conducted in a 10 mm path length cuvette. Absorption and emission spectra were recorded on Shimadzu UV-3600 UV-VIS-NIR and Horiba Jobin Yvon Fluorolog spectrometers, respectively. NIR emission spectra were recorded using an EDINBURGH FLS1000 spectrometer. Quantum yields were measured using an integrating sphere in the same instrument by exciting at 600 nm. The fluorescence lifetime measurements in hexane were carried out in an IBH picosecond time-correlated single-photon counting (TCSPC) system. The pulse width of the excitation (λ_{ex}=640 nm) source is determined to be <100 ps. The fluorescence decay profiles were de-convoluted using DAS6.3 and fitted with exponential decay, minimizing the χ^2 values. The emission decay measurements in THF and ACN were unsuccessful due to the lack of photon collection efficiency of the detector beyond 970 nm, which resulted in poor photon count.

Radiative (k_r) and non-radiative (k_{nr}) decay rate constants can be calculated by using the equation.[1, 2]

$$\varphi_{Fl} = \frac{k_r}{k_r + k_{nr}} \quad \text{S1}$$

$$\tau = \frac{1}{k_r + k_{nr}} \quad \text{S2}$$

$$k_r = \frac{1}{k_r + k_{nr}} \quad \text{S3}$$

$$k_{nr} = \frac{1}{\tau} - k_r \quad \text{S4}$$

Stokes shift in cm^{-1} is calculated using the equation

$$\Delta E = hc[\frac{1}{\lambda 1} - \frac{1}{\lambda 2}] \quad \text{S5}$$

Where, h = Planck constant

c = Speed of light

λ_1 = Absorption maximum

λ_2 = Emission maximum

1.1 Computational Analysis

All the calculations were carried out in Gaussian 16.[3] Ground-state geometry optimization in vacuum performed at CAM-B3LYP/def2svp level of theory. The frontier molecular orbitals (FMO) were obtained from the generated cube files of energy calculations. Vertical excitation energies and oscillator strengths were calculated employing time-dependent DFT (TD-DFT) at the CAM-B3LYP/def2svp level of theory. Geometry optimization of the first singlet excited-state (S_1) was carried out employing CAM-B3LYP functional and def2svp basis set. Hole-electron isosurfaces and NTO analysis for the TDI-TPA$_4$ system were generated using Multiwfn 3.8.[4] Visualization states were rendered using VMD 1.9.3 software.

1.2 TheoDORE Analysis

The nature of the excited states in TDI-TPA_4 was analyzed using TheoDORE at the ground-state optimized geometry.[5, 6] TDI core and triphenylamine unit are considered two fragments (Figure S26). The parameters used to investigate the excited-state characteristics are participation ratio (PR), mean position (POS) of initial orbital (hole) and final orbital (electron), and charge transfer character (CT). The magnitude of PR relates to the number of fragments participating in the excitation; hence, in our investigation, the PR ranges from 1 to 3. POS provides the mean position of the hole and electron for a particular excitation. Finally, CT is related to the total weight of configurations where initial and final orbitals are situated on different fragments. CT>0.8 denotes charge transfer state and CT=0 Frenkel exciton state (FE). Further, electron-hole correlation plots were generated to give a qualitative picture of the character of each state in TDI-TPA_4.

1.3 Femtosecond Transient Absorption (fsTA) Measurement

A Spectra-Physics Mai Tai SP mode-locked laser, with an operating frequency of 86 MHz and emitting light at 800 nm, served as the seed for a Spectra-Physics Spitfire ace regenerative amplifier. The regenerative amplifier operated at a repetition rate of 1 kHz and produced an output energy of 5.5 mJ. A fraction of the amplified output was utilized to generate a 520 nm pump pulse through TOPAS. Simultaneously, the remaining 800 nm pulse underwent an optical delay within an ExciPro pump-probe spectrometer. A sapphire crystal introduced into this path generated a white light continuum, which was then split into two streams, serving as probe and reference pulses. Femtosecond transient absorption spectra of the sample were captured using a dual diode array detector with a detection window of 200 nm and an optical delay of 3.5 ns. Sample solutions housed in a rotating cuvette with a path length of 1.2 mm were employed for recording. To enable accurate deconvolution of the transient absorption data, an instrument response function (IRF) was determined. The IRF, established through a solvent (10% benzene in methanol) two-photon absorption, was approximately 110 fs at around 530 nm. An 80% neutral density filter regulated incident flux on the sample. For the fsTA measurement of TDI-TPA_4, the sample was excited with 520 nm, 200 nJ, and 100 fs pulses. The observed kinetic components were independent of laser intensity, eliminating the possibility of singlet–singlet annihilation.[7]

Sample preparation for thin film fsTA analysis: For the fsTA thin film measurements, a round quartz cuvette has been cleaned by following standard cleaning protocols.[8] Followingly, TDI-TPA_4 (10 mg/mL) dissolved in polystyrene in toluene (20 mg/mL) uniformly dropcasted on the quartz cuvette.

The ensemble level fsTA measurements of TDI-TPA_4 in PVA polymer films were performed by drop-casting of the PVA solution in water and TDI-TPA_4 in toluene onto the precleaned quartz cuvette to prevent any aggregation of the sample in the PVA matrix. A freshly prepared mixture of polyvinyl alcohol (2 mg/mL) and glycerol (10 μL) in distilled water was stirred at 90°C for 1 h and dropcasted on the quartz cuvette. The sample solution of TDI-TPA_4 (10 mg/mL) was prepared in toluene and dropcasted on a dried PVA layer. The films were dried in a vacuum and stored in a nitrogen atmosphere prior to the experiments.

The magic angle polarization ~54.7°, between pump and probe pulses used to ensure an isotropic signal of the sample.

1.4 Nanosecond Transient Absorption (nsTA) Measurement

Nanosecond laser flash photolysis measurements were carried out on a nitrogen-purged solution of TDI-TPA_4 in toluene, tetrahydrofuran, and acetonitrile. These experiments employed an Applied Photophysics Model LKS-60 laser kinetic spectrometer, where the third harmonic (532 nm, pulse duration

approximately 10 ns) of a Quanta Ray INDI-40-10 series pulsed Nd:YAG laser served as the excitation source.

1.5 Electrochemistry

Cyclic voltammograms and differential pulse voltammograms were acquired on CH instruments, inc electrochemical workstation at room temperature, employing a three-electrode single-compartment cell: glassy carbon electrode as the working electrode, a Pt wire as the counter electrode, and silver wire as the reference electrode. Working and reference electrodes were polished on a felt pad with 0.05 μm Al_2O_3 suspension, sonicated in acetone for about 3 minutes, and dried before each experiment; the Pt wire was flame-cleaned. The supporting electrolyte, tetrabutylammonium hexafluorophosphate (TBAF), was previously dried under vacuum, dichloromethane was degassed prior to use, and all measurements were performed under a nitrogen atmosphere. The concentration of TBAF used was typically 100 times the analyte. Calibration of the instrument was performed using the ferrocene/ferrocenium (Fc/Fc^+) redox couple as an external standard and measured under the same condition before and after the measurement of samples. $E_{Fc/Fc+}$ is the potential of Fc/Fc^+ vs. Ag (0.51 V, as measured by cyclic voltammetry).[9] The energy level of Fc/Fc+ was assumed to be –4.8 eV with respect to vacuum.[10] HOMO and LUMO energies were calculated using the following equation.

$$E_{HOMO} = -(E_{OX} + 4.8\text{-}E_{Fc/Fc+})\ \text{eV} \quad \text{S6}$$

$$E_{LUMO} = -(E_{red} + 4.8\text{-}E_{Fc/Fc+})\ \text{eV} \quad \text{S7}$$

respectively, where E_{ox} and E_{red} are the experimentally measured oxidation and reduction potentials vs. Ag.

The electrochemical energy gap (Eg) is estimated as follows:

$$\boldsymbol{E_g = (E_{LUMO}\text{-}E_{HOMO})} \quad \text{S8}$$

Where E_{LUMO} and E_{HOMO} are the corresponding to LUMO and HOMO energy levels.

1.6 Global Analysis

The fsTA spectra underwent global analyses using Glotaran software.[11] This process involved assessing the instrument time response function and the group velocity dispersion of the white continuum, enabling the computation of decay time constants and dispersion-compensated spectra. In global analysis, all wavelengths were simultaneously scrutinized, utilizing a sequential model to generate evolution-associated spectra (EAS). It is crucial to note that EAS illustrates the temporal evolution of the spectra and may not necessarily represent genuine physical or chemical species. Instead, EAS signifies the spectral changes occurring with their corresponding time constants.

1.7 Electrode Preparation for Spectroelectrochemistry

Fluorinated tin oxide (FTO) substrates were cleaned by 15-minute ultrasonication steps using soap solution, water, isopropanol, and acetone, in sequence. The FTO glasses were then sandwiched using a double-sided tape. The solution containing TDI-TPA_4 was poured into the gap between the transparent glass electrodes.

1.8 Redox Titration

The redox titration measurements for TDI-TPA_4 were carried out to comprehend the evolution of radical anion and cation upon photoexcitation. Chemical reduction experiments of the TDI-TPA_4 were carried out with a minimum amount of antimony pentachloride ($SbCl_5$). Chemical reduction of the TDI-TPA_4 was achieved using cobaltocene as the reducing agent.

1.9 Rehm-Weller Analysis

The free energy change for the charge separation (ΔG_{CS}) and charge recombination (ΔG_{CR}) were calculated employing the following relations built on the Born dielectric continuum model.

$$\Delta G_{CS} = e[E_{ox} - E_{red}] - E_{00} + C + S \quad \text{S9}$$

$$C = \frac{-e^2}{4\pi\epsilon_0}\left(\frac{1}{\epsilon_S r_{AD}}\right) \quad \text{S10}$$

$$S = \frac{e^2}{4\pi\epsilon_0}\left(\frac{1}{r_D} + \frac{1}{r_A}\right)\left(\frac{1}{\epsilon_S} - \frac{1}{\epsilon_{SP}}\right) \quad \text{S11}$$

$$\Delta G_{CR} = -(E_{00} + \Delta G_{CS}) \quad \text{S12}$$

Where e is the charge of the electron, E_{ox} and E_{red} are the oxidation and reduction potentials, respectively, ϵ_0 is the permittivity of free space, ϵ_S is the static dielectric constant of the solvent, and ϵ_{SP} is the static dielectric constant of the solvent used for electrochemical measurements, r_{AD} is the donor-acceptor distance, r_D and r_A are the cation and anion hard-sphere radii, respectively (were approximated as $r_{AD}/_2$) and E_{00} is the energy of the excited singlet (donor) state. At finite distances, the Coulombic attraction energy between (C) and the radical ion is given by a point-charge model as ($1/\epsilon_S r_{AD}$). In the polar solvents, the optical bandgap (E_{00}) was determined by the intersection of the normalized absorption and emission spectra of TDI-TPA_4 in hexane.

1.10 Single-Molecule Fluorescence Measurements

Fluorescence lifetime imaging microscopy (FLIM) images and fluorescence intensity trajectories (FITs) were obtained using the MicroTime 200 (MT200) time-resolved fluorescence microscope by PicoQuant. The inverted microscope (Olympus IX83) was equipped with a piezo scanning stage (P-733.2CD, PI). Sample excitation was achieved using a 512 nm pulsed laser (LDH-D-C-512, PicoQuant) with a repetition rate of 20 MHz, and scanning was performed with a dwell time of 0.4 ms. A water immersion objective (UplanSApo 60× NA 1.2) collected the photons. Spectral filtering utilized a major dichroic mirror (zt405-442/510 rpc-UF3, Chroma) and a 519 nm long-pass emission filter (FF01-519/LP, Semrock). A pinhole (50 μm) spatially filtered the photons, which were then directed to a SPCM-AQRH single-photon avalanche photodiode (SPAD) detector. The detector signals underwent postprocessing by the HydraHarp 400 time-correlated single-photon counting (TCSPC) data acquisition unit (PicoQuant). SymPhoTime64 software (PicoQuant) handled data recording and analysis. A mixture of TDI-TPA_4 (~10^{-10} M) and a polystyrene matrix (2% w/v) in toluene was spin-coated on a plasma-cleaned coverslip of 0.13-0.16 mm thickness. A freshly prepared mixture of polyvinyl alcohol (2 mg/mL) and glycerol (10 μL) in distilled water was stirred at 90°C for 1 h. The sample solution of TDI-TPA_4 was prepared in toluene (~10^{-12} M). The thin film was prepared by sandwiching the sample layer by alternatively spin coating the polymer solution. After preparation, the thin film sample was placed in a vacuum for 10 minutes (Figure S39).[12] Fluorescence lifetimes and FITs of TDI-TPA_4 single molecules were obtained by exciting the sample at 512 nm (refer to Figures S29 and S30). The excitation laser operated at a repetition rate of 20 MHz with a power of ~0.12 μW. Fluorescence lifetimes and FITs with a 10 ms bin time were acquired using SymPhoTime software. Photon antibunching measurements were conducted using the standard Hanbury Brown-Twiss interferometer configuration in the MicroTime200 from PicoQuant using an 800 nm short-pass filter. The intensity threshold was set based on the background signal in the PS-coated coverslip. Fluorescence intensity above the threshold was considered the "on" state, while intensity below the threshold was considered the "off" state. Polystyrene (PS) and polyvinyl alcohol (PVA) matrices were procured from Sigma-Aldrich.

Section 2: Syntheses and Characterization

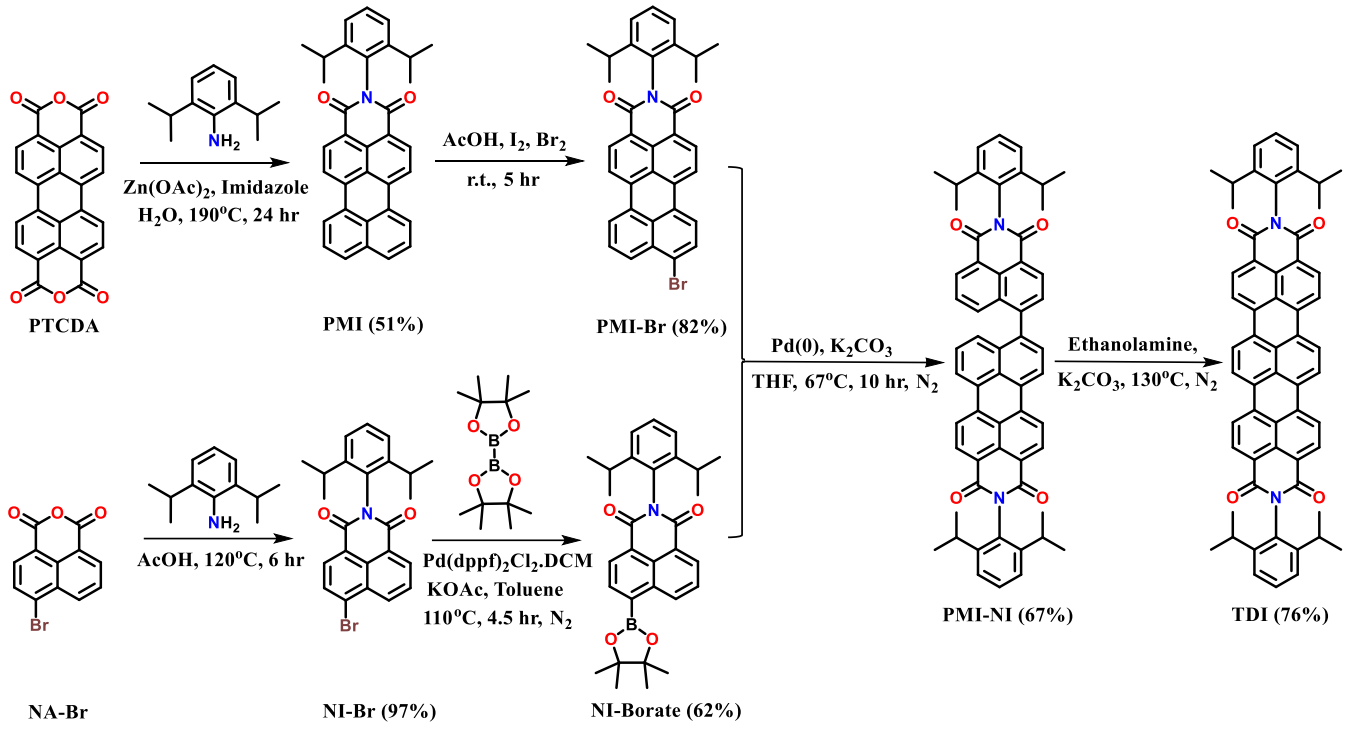

Scheme S1: Synthesis scheme of TDI.

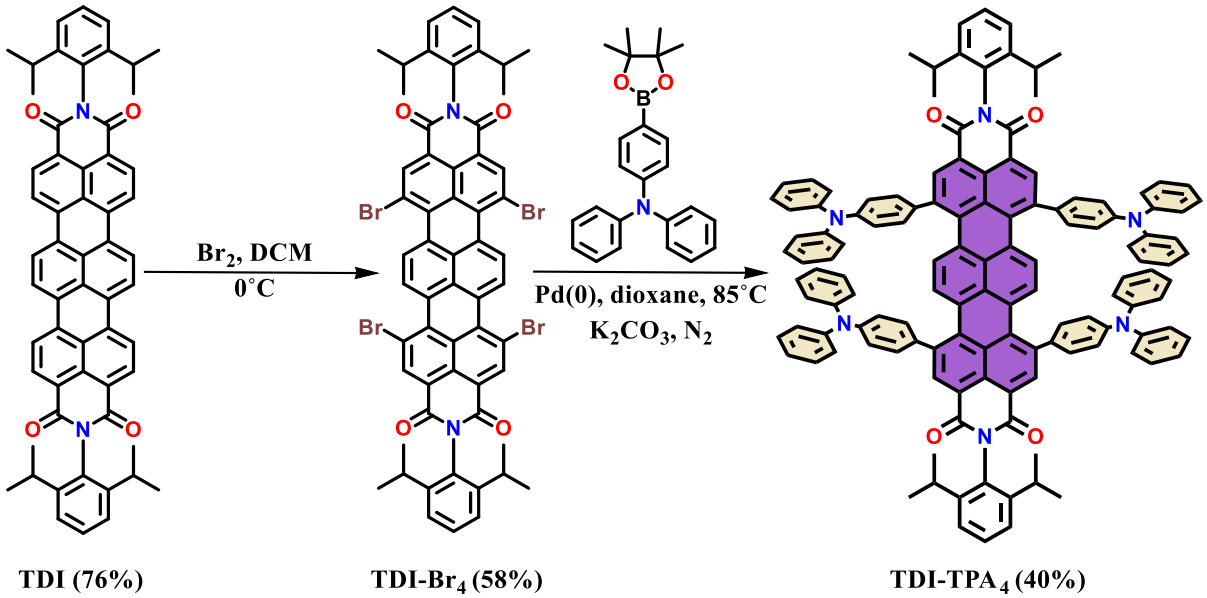

Scheme S2: Synthesis scheme of TDI-TPA4.

2.1 Synthesis of PMI

A mixture of 3,4,9,10-tetracarboxylic dianhydride (PTCDA) (3.66 g, 9.34 mmol), 2,6-diisopropylaniline (0.91 g, 5.12 mmol), zinc acetate (1.32 g, 7.19 mmol) and imidazole (18.70 g, 274.70 mmol) in 8 mL water was heated at 190°C in an autoclave for 23 h. The reaction mixture was extracted by chloroform

and filtered through celite. The filtrate was then washed with dilute HCl and water, and solvents were removed under reduced pressure. Further purification was done using column chromatography (silica gel, DCM: petroleum ether 3:2) to yield a brown-red residue (51% yield).

^{1}H NMR (500 MHz, $CDCl_3$, ppm): δ = 8.58-8.56 (d, J = 5 Hz, 2H), 8.38-8.34 (t, J = 8H z, 4H), 7.84-7.82 (d, J = 8 Hz, 2H), 7.58-7.54 (t, J = 8 Hz, 2H), 7.43-7.39 (t, J = 8 Hz, 1H), 7.28-7.27 (d, J = 8 Hz, 2H), 2.73-2.68 (m, 2H), 1.12-1.11 (d, J = 7Hz, 12H)

HRMS (APCI) m/z calculated for $C_{34}H_{27}NO_2$ (m/z):$[M+H]^+$ = 482.2115; Found:482.2105

2.2 Synthesis of PMI-Br

PMI (1.9 g, 3.95 mmol) and Iodine (1.9 g, 481.58 mmol) in catalytic amounts were dissolved in acetic acid with moderate heating. To this solution, bromine (1.26 g, 15.78 mmol) was added, and the reaction mixture was heated for 5 hours. Unreacted bromine was quenched using a saturated solution of sodium thiosulphate. The organic layer was extracted using water and DCM. The obtained organic layer was concentrated under a vacuum, and the residue was purified by column chromatography (silica gel, DCM: petroleum ether 2:3) to yield 82% as a bright red solid.

^{1}H NMR ((500 MHz, $CDCl_3$, ppm): δ = 8.59-8.56 (t, J = 8 Hz, 2 H), 8.39-8.36 (m, 2H), 8.32-8.31 (d, J = 8 Hz, 1H), 8.23-8.21 (d, J = 8 Hz, 1H), 8.15-8.13 (d, J = 8 Hz, 1H), 7.8-7.81 (d, J = 8 Hz, 1H), 7.65-7.62 (t, J = 8 Hz, 1H), 7.43-7.40 (t, J = 8 Hz, 1H), 7.29-7.2 (d, J = 8 Hz, 2H), 2.72-2.69 (t, J = 7 Hz, 2H), 1.13-1.11 (d, J = 7 Hz, 12H)

HRMS (APCI) m/z calculated for $C_{34}H_{26}BrNO_2$ (m/z):$[M+H]^+$ = 560.1220; Found:560.1207

Synthesis of NI-Br

In a round bottom flask, 4-Bromo-Naphthalene-1,8-dicarboximide (5.5 g, 19.85 mmol) and 2,6-diisopropylaniline (7.038 g, 39.7 mmol) are taken, 110 mL of acetic acid is poured into it and was kept it at 120°C with stirring for six hours. Reaction stopped after the full consumption of starting material using thin-layer chromatography, and the respective compound was purified using column chromatography (silica gel, DCM: petroleum ether 1:20) to yield a white solid yield of 97%.

^{1}H NMR (500 MHz, $CDCl_3$): δ (ppm) 8.71 (d, J = 7.2 Hz, 1H), 8.65 (d, J = 8.4 Hz, 1H), 8.47 (d, J = 7.6 Hz, 1H), 8.09 (d, J = 7.6 Hz, 1H), 7.89 (t, J = 8.4 Hz, 1H), 7.46 (t, J = 7.6 Hz, 1H), 7.31 (d, J = 8.0 Hz, 2H), 2.66 (m, 2H), 1.14 (d, J = 6.8 Hz, 12H).

HRMS (APCI) m/z calculated for $C_{24}H_{22}BrNO_2$ (m/z):$[M+H]^+$ = 436.0834; Found:436.0724

Synthesis of NI-Borate

NI-Br (1.6 g, 3.66 mmol), Bis-(pinacolato)-diboron (1.77 g, 6.97mmol), potassium acetate (1.083 g, 10.998 mmol) and palladium(0) (306.08 g, 0.37mmol) catalyst were put together and kept in vacuum for 20 minutes. Toluene was added to this, followed by the purging of Nitrogen gas for 30 minutes. The reaction mixture was kept for reflux at 110°C for 4.5 hours. After the product formation and reaction, the mixture was allowed to room temperature, and the solvent was removed using a rotary evaporator. Product purified by column chromatography (silica gel, Ethyl acetate: petroleum ether 1:10) to yield 62% white powder.

^{1}H NMR (500 MHz, $CDCl_3$, ppm): δ = 9.15-9.13 (d, J = 8.5 Hz, 1H), 8.60-8.55 (t, J = 7 Hz, 2H), 8.29-8.27 (d, J = 7.5 Hz, 1H), 7.78-7.75 (t, J = 7.5 Hz, 1H), 7.39-7.38 (t, J = 7.5 Hz, 1H), 7.26-7.25 (d, J = 7.5Hz, 2H), 2.72-2.69 (m, 2H), 1.39 (s, 12H). 1.19 (s, 12H)

HRMS (APCI) m/z calculated for $C_{30}H_{34}BNO_4$ (m/z):$[M+H]^+$ = 484.2654; Found:484.2651

Synthesis of PMI-NI

PMI-Br (1.54 g, 2.76 mmol), potassium carbonate (2.86 g, 20.69 mmol), and NI Borate (2 g, 4.14 mmol) were weighed in a two-neck round bottom flask and kept vacuum for 20 minutes. 140 mL of THF, 45 mL water, and (tetrakis(triphenylphosphine)palladium(0) 0.238 g, 0.206 mmol) were added under inert

conditions, followed by heating at 67°C for 10 hours in a nitrogen atmosphere. The solvent was removed under reduced pressure, and the residue was purified by column chromatography (silica gel, DCM: petroleum ether 2:3)

^{1}H NMR (500 MHz, $CDCl_3$, ppm): δ = 8.66-8.65 (d, J = 8.5 Hz, 1H), 8.60-8.59 (d, J = 8 Hz 3H), 8.54 (s, 2H), 8.49 (s, 2H), 2.81-2.67 (m, 4H), 1.14-1.18 (d, J = 6.5, 24H)

HRMS (APCI) m/z calculated for $C_{58}H_{48}N_2O_4$ (m/z):$[M+H]^+$= 837.3614; Found:837.3669

Synthesis of TDI

PMI-NI (1g 1.19 mmol) and K_2CO_3 (8.25 g, 59.7 mmol) were stirred in ethanolamine (11.26 g, 184.34 mmol) for 4.5 hours at 160°C. After cooling down to room temperature, the solution was poured into methanol and then centrifuged. The supernatant was discarded, and the pellet was dried under vacuum and purified by column chromatography (DCM: Pet ether 1:10) to yield 76% of the blue-colored product.

^{1}H NMR (500 MHz, $CDCl_3$, ppm): δ = 8.69-8.68 (d, J = 7.5 Hz, 8H), 8.59 (s, 4H), 7.43 (s, 2H), 7.3-7.29 (d, J = 5.5 Hz, 4H), 2.71 (s, 4H), 1.12 (s, 24H)

HRMS (APCI) m/z calculated for $C_{58}H_{46}N_2O_4$ (m/z):$[M+H]^+$ = 835.3530; Found:835.3523

Synthesis of TDI-Br$_4$

TDI (800 mg, 0.96 mmol) in 180 mL dichloromethane stirred for 30 minutes at 0°C. Followed by 3.2 mL Br_2 in 17.6 mL DCM solution, added dropwise over a time of 30 minutes. The reaction was stopped after full consumption of the starting material. Excess bromine was quenched with saturated with sodium thiosulphate. The organic phase was extracted with dichloromethane dried over anhydrous Na_2SO_4, and the solvent evaporated under reduced pressure. The pure blue color product resulted after column chromatography (silica gel, DCM: petroleum ether 1:5) (58%).

^{1}H NMR (500 MHz, $CDCl_3$, ppm): δ = 9.49 (s, 2H) 9.38-9.42 (2H), 8.68 (d, 8H), 8.94 (s, 2H), 8.75 (s, 2H), 7.47-7.44 (2H), 7.31-7.30 (d, J = 5.5 Hz, 4H), 2.69-2.64 (m, 4H), 1.12 (s, 24H)

HRMS (APCI) m/z calculated for $C_{58}H_{42}N_2O_4Br_4$ (m/z):$[M+H]^+$ = 1149.9832 Found:1149.9853

Synthesis of TDI-TPA$_4$

TDI-Br_4 (100 mg, 0.09 mmol), 4-(diphenylamino)phenylboronic acid (370 mg, 1.28 mmol), and potassium carbonate (176.90 mg, 1.28 mmol) weighed in a schlenk tube, kept vacuum for 20 minutes and nitrogen flushed 3 times. 10 mL dioxane and 3 mL water followed by (tetrakis(triphenylphosphine)palladium(0) added under nitrogen atmosphere. In order to remove the complete presence of oxygen freeze-pump-thaw has been carried out twice. The reaction mixture was heated to 85°C for 16 hours. After the completion of the reaction, the organic phase was extracted with dichloromethane dried over anhydrous Na_2SO_4, and the solvent evaporated under reduced pressure. The pure purple color product resulted after column chromatography using ethyl acetate/hexane, 1:10 as eluent with a 40% yield

^{1}H NMR (500 MHz, THF-D8, ppm): δ = 8.63 (s, 4H), 7.74 (s, 4H), 7.50-7.44 (dd, 10H), 7.37-7.35 (d, 4H), 7.32-7.29 (t, 16H), 7.20-7.19 (d, J = 5, 8H), 7.15-7.14 (d, J = 5, 16H), 7.05-7.02 (t, 8H, J = 10), 2.90-2.84 (m, 4H), 1.21 (s, 24H)

^{13}C NMR (126 MHz, THF-D8, ppm): δ = 163.7, 148.5, 147.9, 146.2, 140.2, 137.6, 135.0, 134.1, 132.0, 130.3, 129.2, 128.6, 125.1, 124.7, 123.8, 121.3, 30.1, 29.5

IR (KBr): cm^{-1} = 1701, 1668, 1591, 1492, 1408, 1350, 1317, 1278, 1024, 856, 813, 754, 698

HRMS (APCI) m/z calculated for $C_{130}H_{98}N_6O_4$ (m/z):$[M+H]^+$ = 1807.7678 Found:1808.7683

Melting point 242.1°C

Section 3: Tables

Table S1: A comparison of organic NIR single-molecule emitters explored in the literature.

Contributed By	Molecule	λ_{max}^{Fl} (nm)	ϕ_{Fl} (%)
Present work	Terrylenediimide (TDI) based donor-acceptor chromophore (TDI-TPA_4)	814	26.2
Müllen, Liu, Li and co-workers	Perylenecarboximide with 2,2-dimetheylpyrimidine J. Am. Chem. Soc., 2024, 146, 7135−7139	732	60
Sandoghdar and co-workers	Dibenzoterrylene (DBT) molecules embedded in p-dichlorobenzene J. Phys. Chem. B, 2023,127,5353−5359	743-745	-
Erker and Basché	Dibenzoterrylene (DBT) J. Am. Chem. Soc., 2022, 144, 14053−14056	741	35
Hammer, Delcamp and co-workers	Series of thienopyrazine-based donor−acceptor−donor J. Org. Chem., 2016, 81, 32−42	748	4.29
Orrit and co-workers	Dibenzoterrylene (DBT) molecules embedded in Naphthalene J. Phys. Chem., 1996, 100, 13892-13894	787	-

Table S2: Concentration-dependent absorption measurement of TDI-TPA$_4$ in THF.

Concentration (mM)	Abs I_O/I_1
0.01	--
0.02	1.44
0.04	1.46
0.06	1.46
0.08	1.46
0.10	1.46
0.15	1.46
0.20	1.45

Table S3: Vertical excitation energies computed at the ground-state optimized geometry of TDI-TPA$_4$ (TD-CAM-B3LYP/def2-SVP level of theory) in vacuum.

State	Oscillator strength (f)	Energy (eV)
S_1	0.63	2.10
S_2	0.06	2.88
S_3	0.21	2.88
S_4	0.004	2.94

Table S4: Oxidation and reduction potential values obtained from cyclic voltammetry measurements of TDI-TPA$_4$ in dichloromethane (DCM).

Solvent	[a]E_{ox}^1 (V)	[a]E_{ox}^2 (V)	[a]E_{ox}^3 (V)	[b]E_{red}^1 (V)	[b]E_{red}^2 (V)	E_{HOMO} (eV)	E_{LUMO} (eV)	E_g (eV)	E_{00} (eV)
DCM	0.44	0.59	0.82	-1.01	-1.14	-5.24	-3.79	1.45	1.57

[a]E_{ox}=– ($E_{ox'}$ – $E_{Fc/Fc+}$) eV, [b]E_{red}=– ($E_{red'}$ – $E_{Fc/Fc+}$) eV, $E_{ox'}$ and $E_{red'}$ is the oxidation and reduction potential vs. Ag, E_{ox} and E_{red} is the oxidation and reduction potential vs. Fc/Fc^+

Section D: Figures

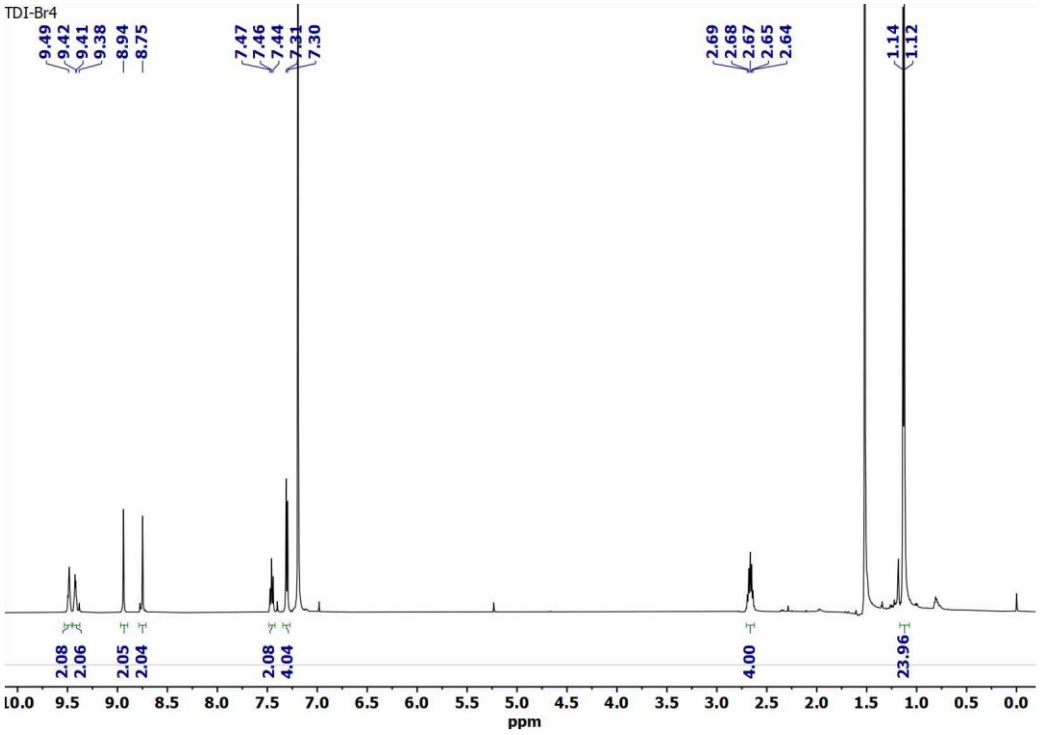

Figure S1: ^{1}H NMR spectrum of TDI-Br_4 in $CDCl_3$.

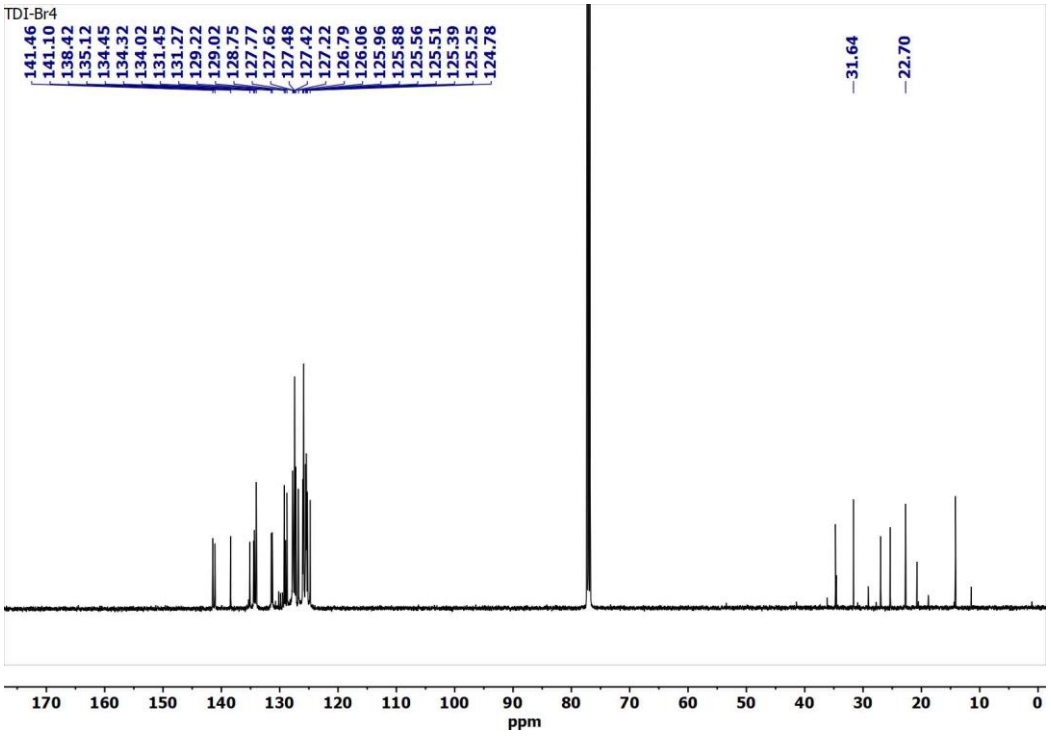

Figure S2: ^{13}C NMR spectrum of TDI-Br_4 in $CDCl_3$.

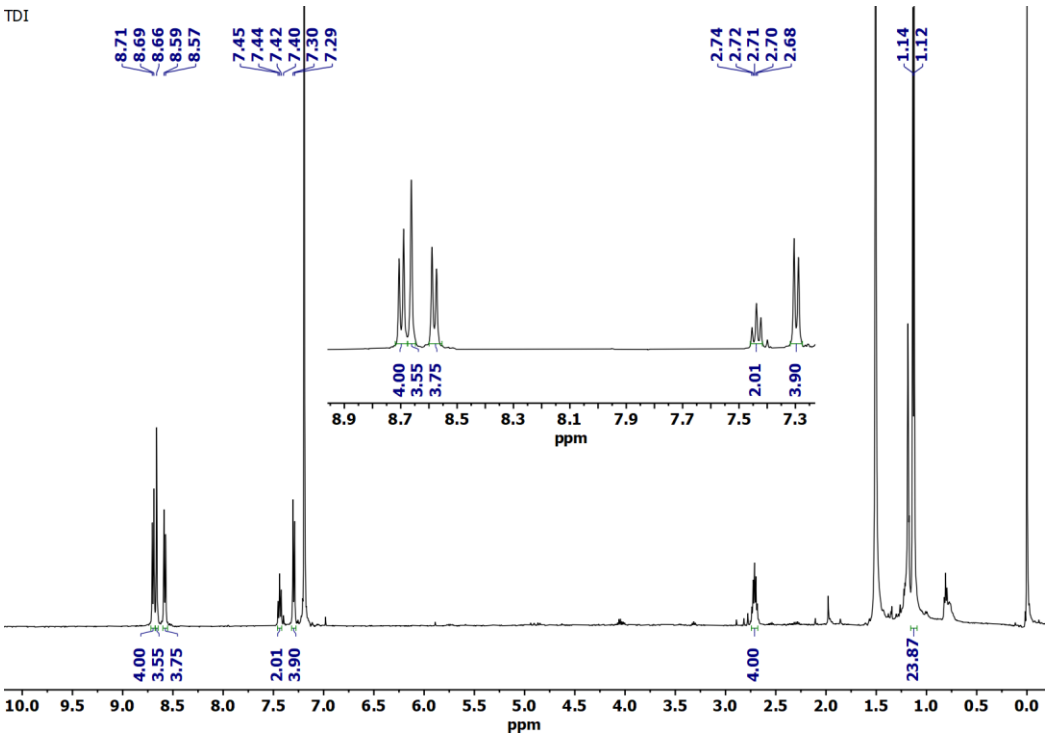

Figure S3: ^{1}H NMR spectrum of TDI in $CDCl_3$.

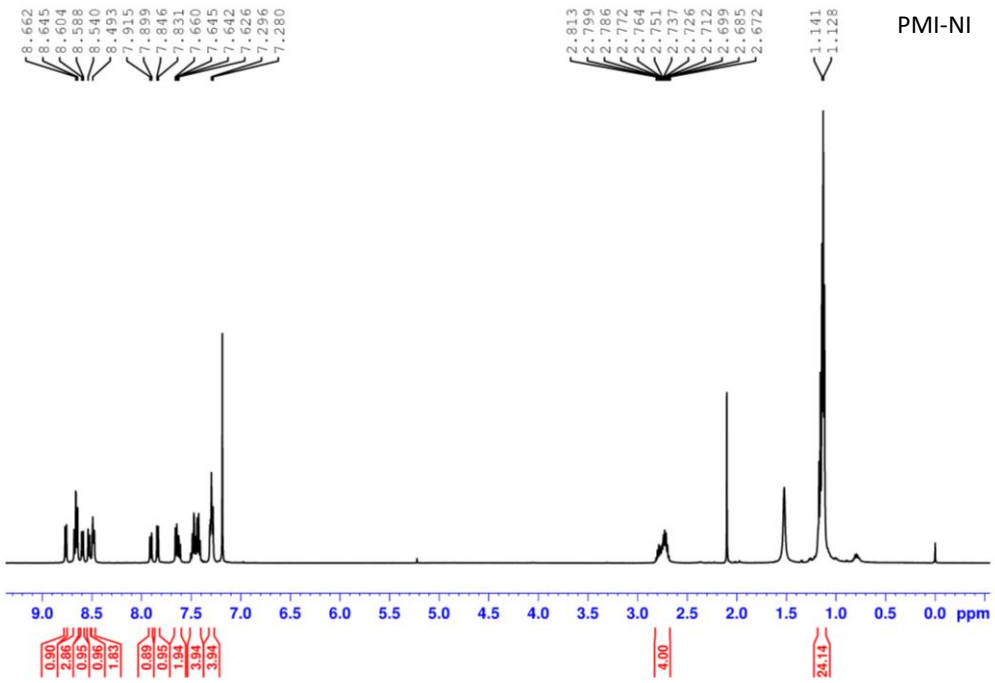

Figure S4: ^{1}H NMR spectrum of PMI-NI in $CDCl_3$.

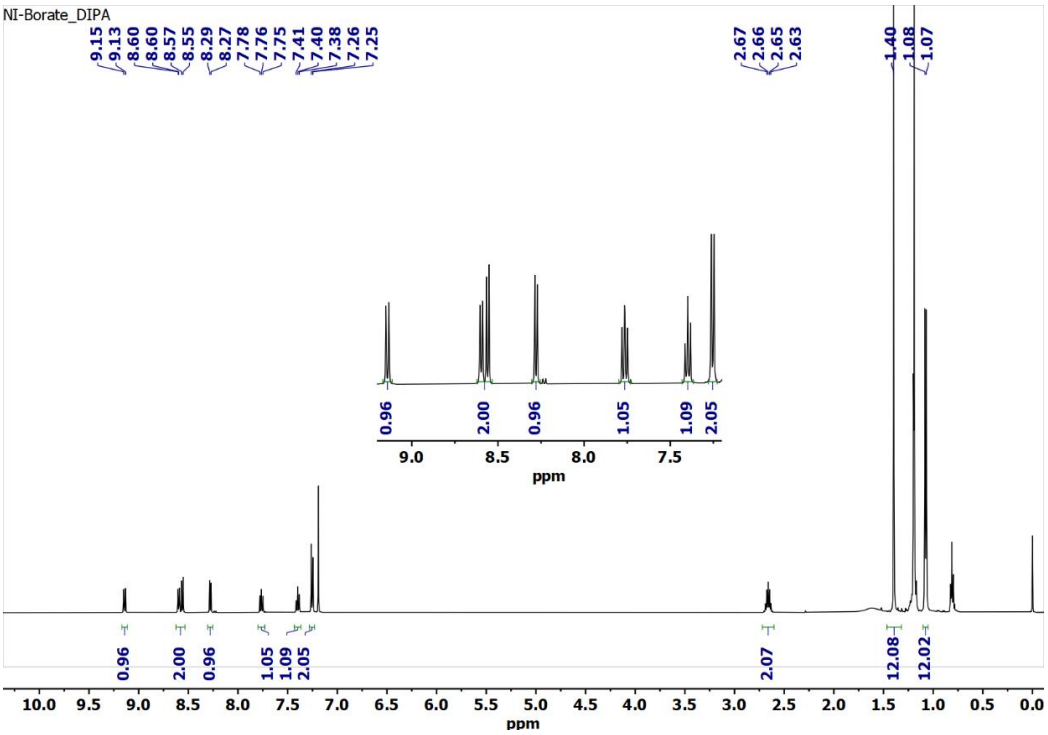

Figure S5: ^{1}H NMR spectrum of NI-Borate in $CDCl_3$.

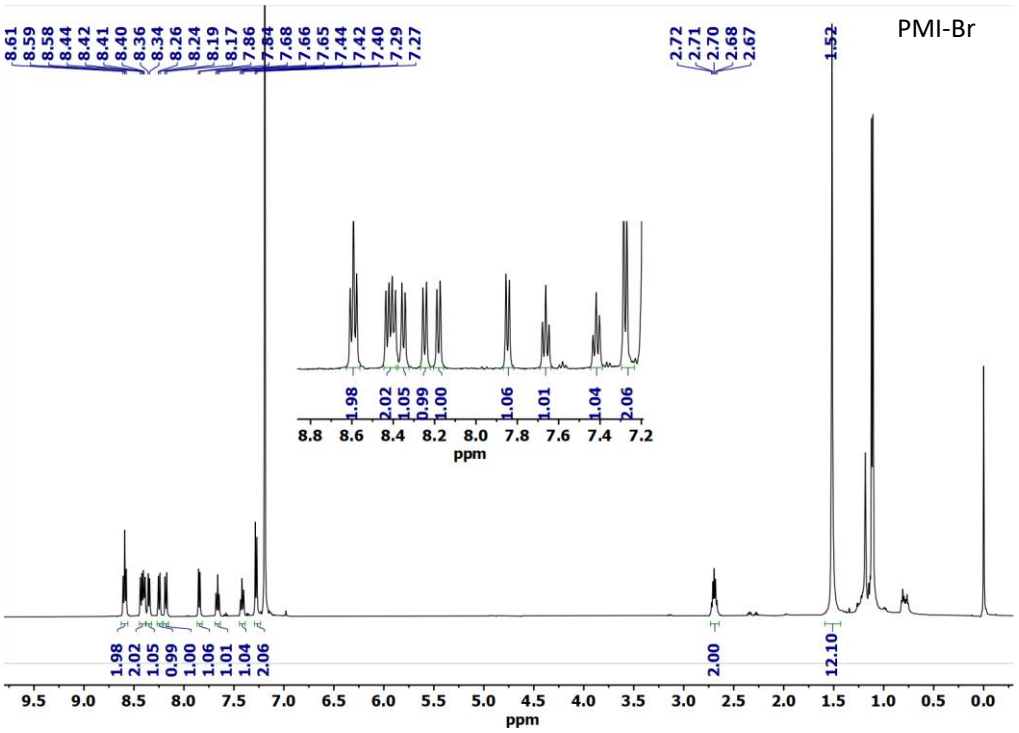

Figure S6: ^{1}H NMR spectrum of PMI-Br in $CDCl_3$.

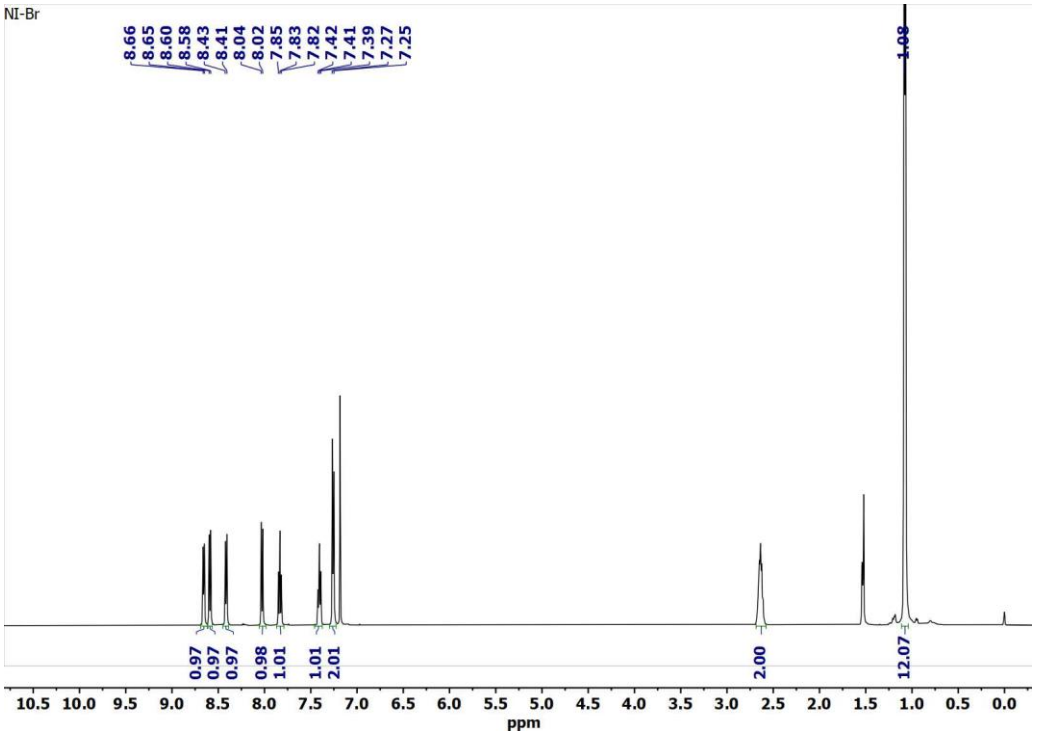

Figure S7: ^{1}H NMR spectrum of Ni-Br in $CDCl_3$.

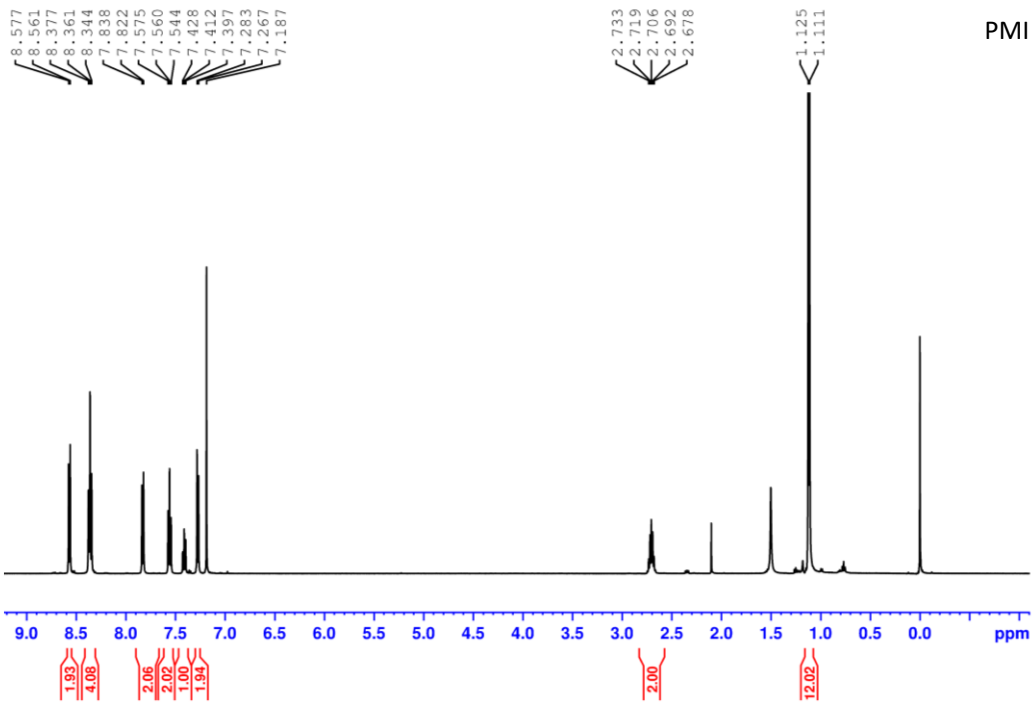

Figure S8: ^{1}H NMR spectrum of PMI in $CDCl_3$.

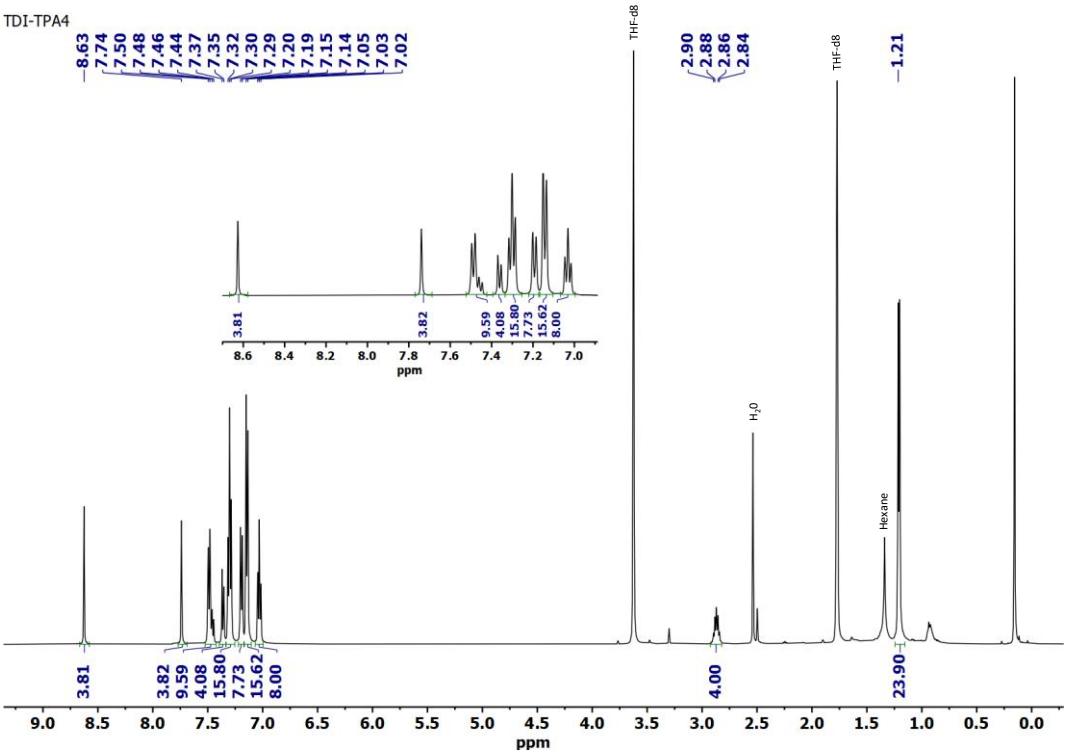

Figure S9: ^{1}H NMR spectrum of $TDITPA_4$ in THF-D8.

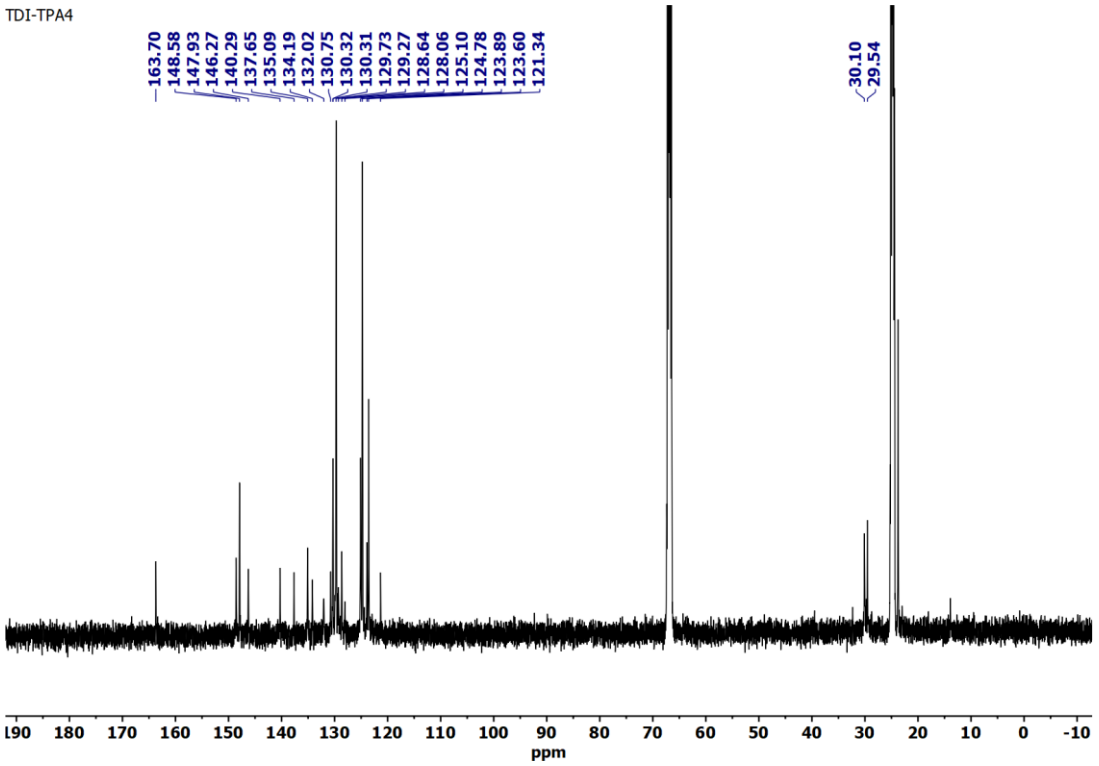

Figure S10: ^{13}C NMR spectrum of $TDITPA_4$ in THF-D8.

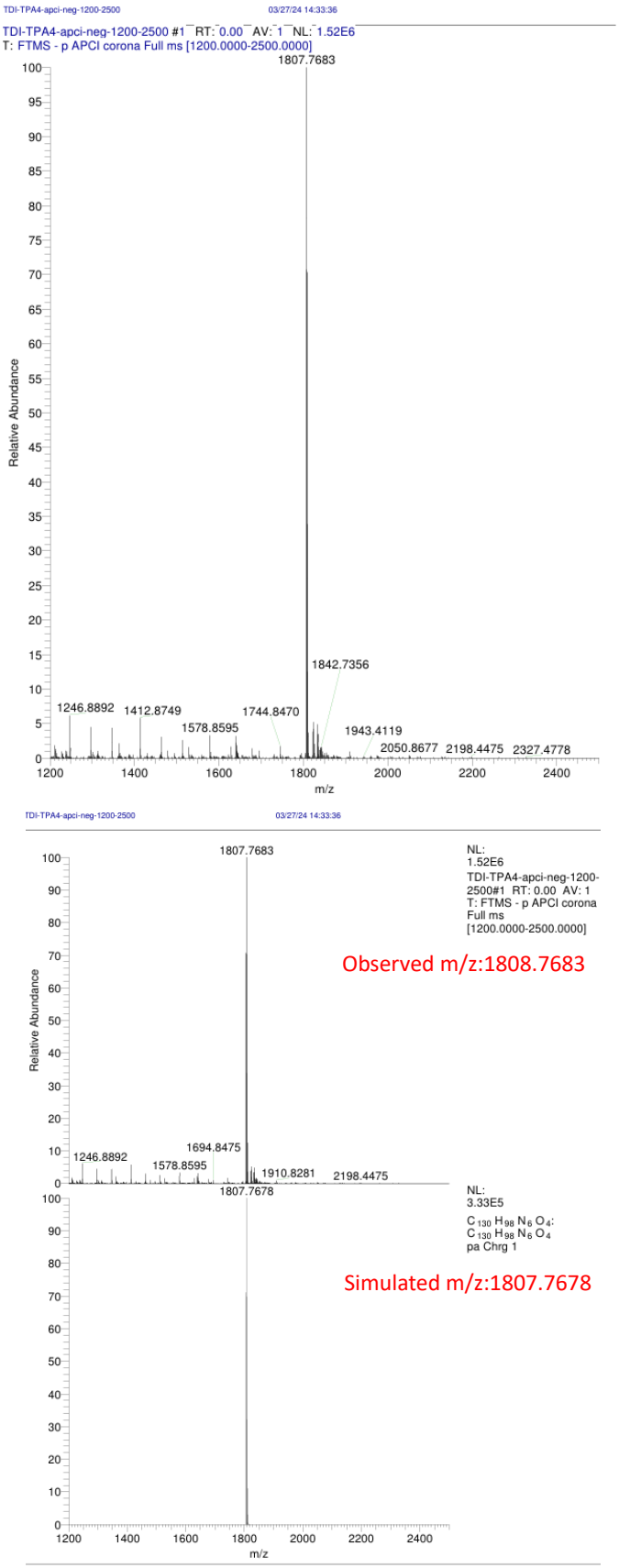

Figure S11: HRMS spectra of TDI-TPA$_4$ with the highlighted molecular mass.

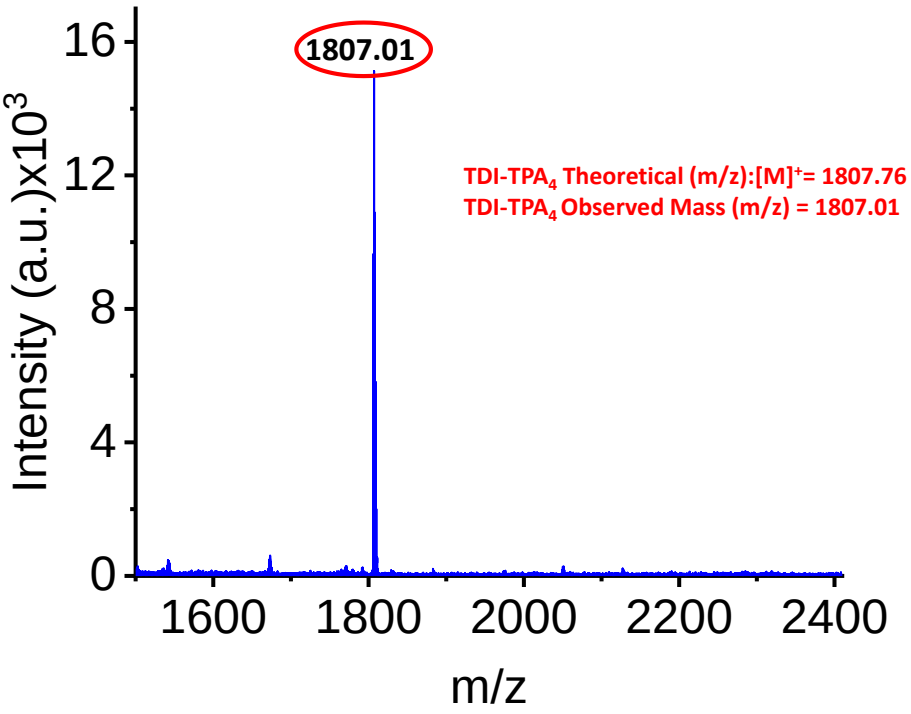

Figure S12: MALDI mass spectrum of TDI-TPA$_4$ with the highlighted molecular mass**.**

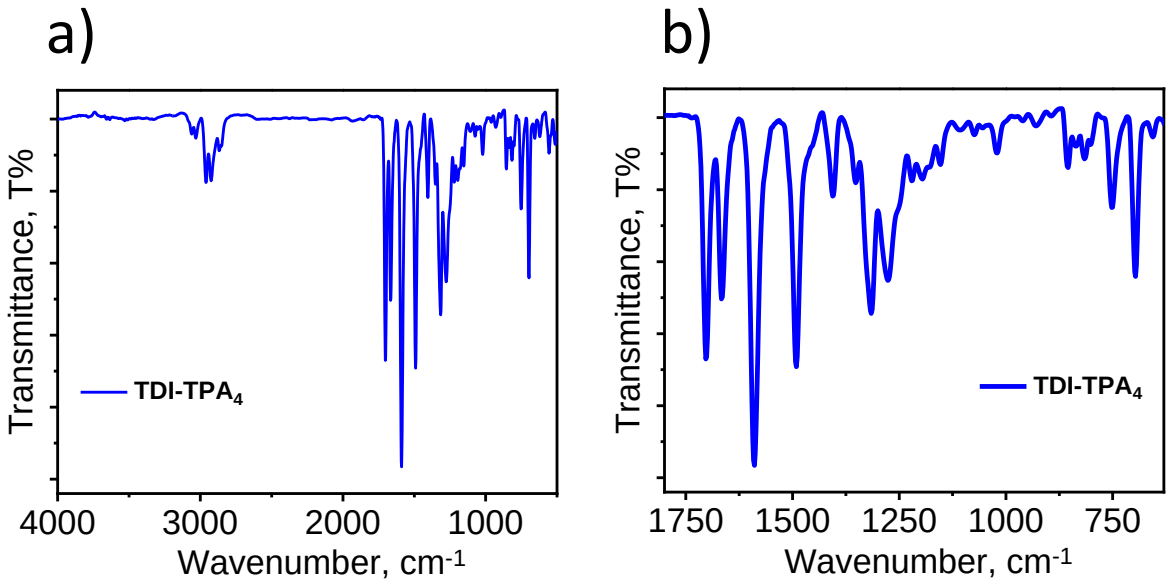

Figure S13: a) The entire FT-IR spectrum of TDI-TPA$_4$ and b) enlarged fingerprint region of TDI-TPA$_4$.

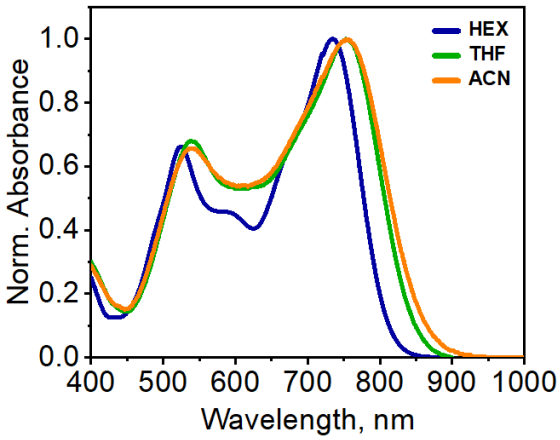

Figure S14: Solvent-dependent normalized UV-vis absorption spectra of TDI-TPA$_4$ in HEX (ε= 1.88), THF (ε = 7.58), and ACN, (ε = 37.5).

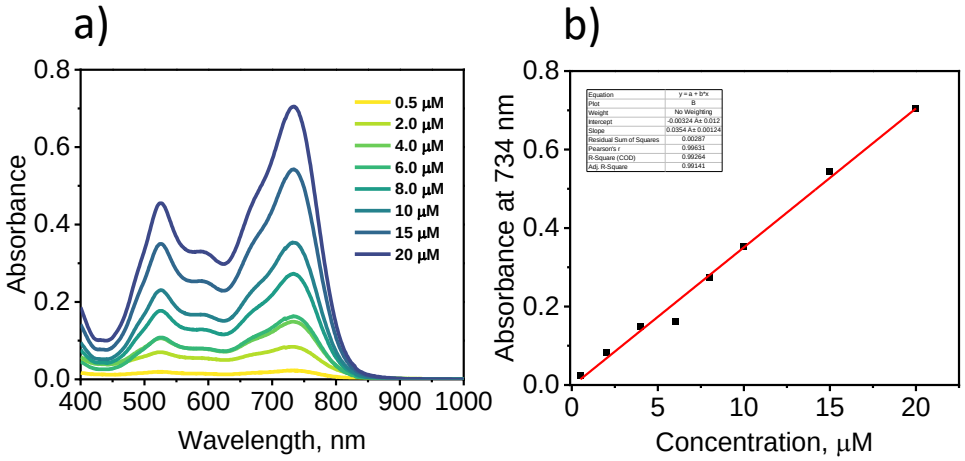

Figure S15: a) Concentration-dependent absorption spectra of TDI-TPA$_4$ in HEX b) Linear plot of absorbance versus concentration at the wavelength 734 nm. Calculated molar extinction coefficient in HEX ε=3.54x10^4 M^{-1}cm^{-1}

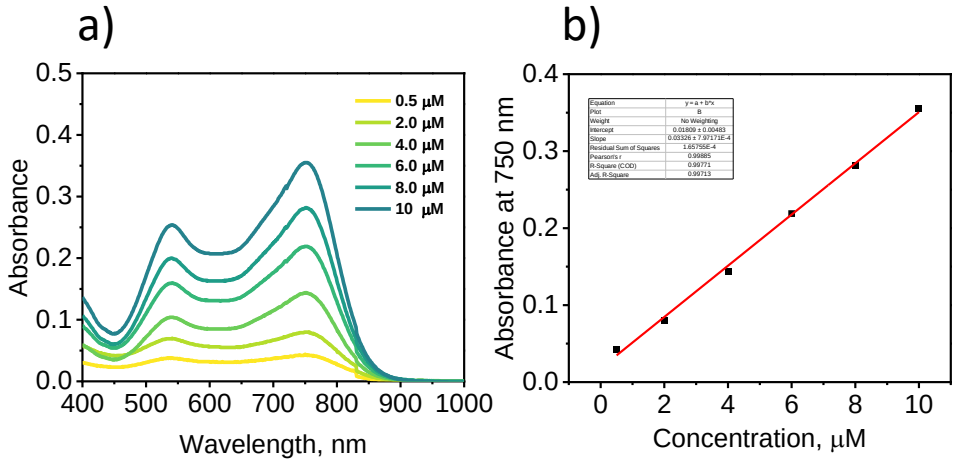

Figure S16: a) Concentration-dependent absorption spectra of TDI-TPA$_4$ in THF b) Linear plot of absorbance versus concentration at the wavelength 750 nm. Calculated molar extinction coefficient in THF ε=3.33x10^4 M^{-1}cm^{-1}

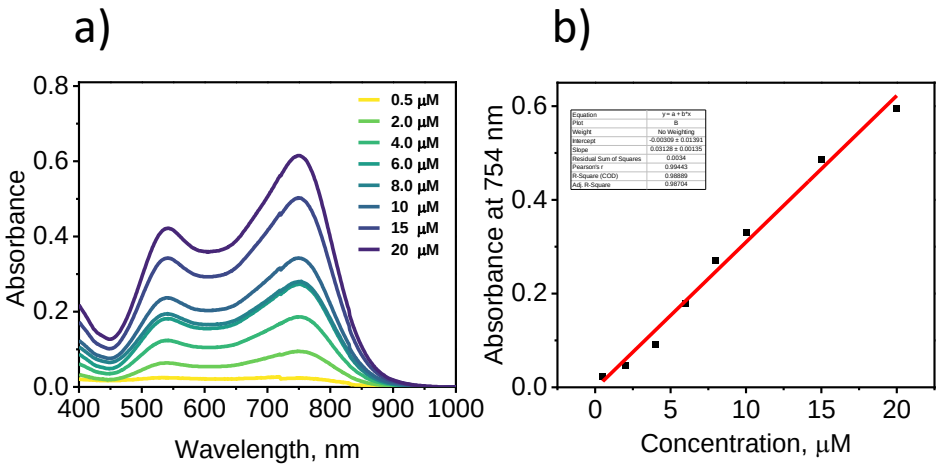

Figure S17: a) Concentration-dependent absorption spectra of TDI-TPA$_4$ in ACN b) Linear plot of absorbance versus concentration at the wavelength 754 nm. Calculated molar extinction coefficient in ACN ε=3.13x10^4 M^{-1}cm^{-1} .

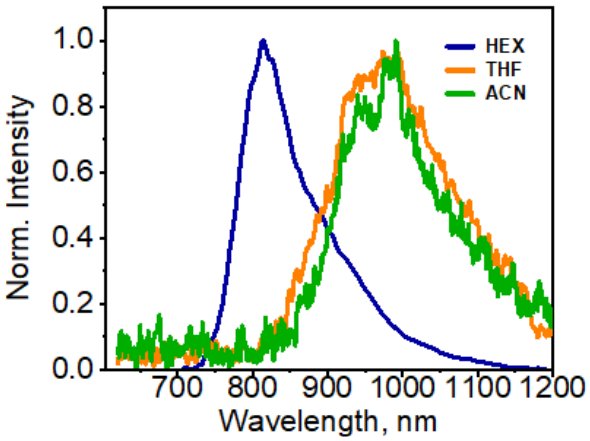

Figure S18: Solvent-dependent normalized emission spectra of TDI-TPA$_4$ in HEX (ε= 1.88), THF (ε = 7.58), and ACN, (ε = 37.5).

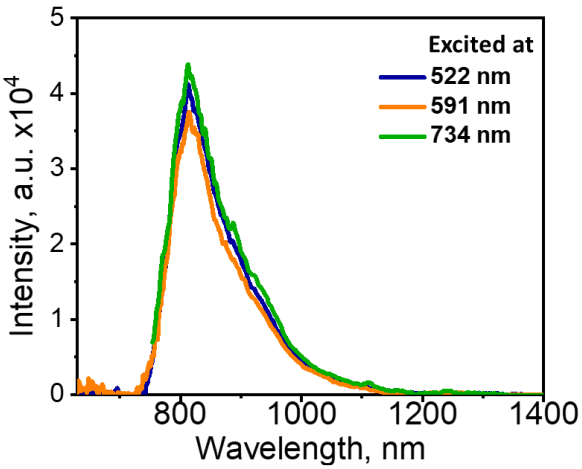

Figure S19: Excitation-dependent emission spectra of TDI-TPA$_4$ in HEX.

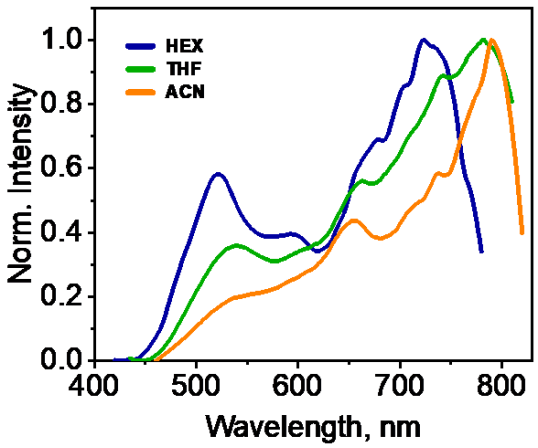

Figure S20: Solvent-dependent normalized excitation spectra of TDI-TPA$_4$ in HEX (ε=1.88), THF (ε=7.58), and ACN, (ε=37.5).

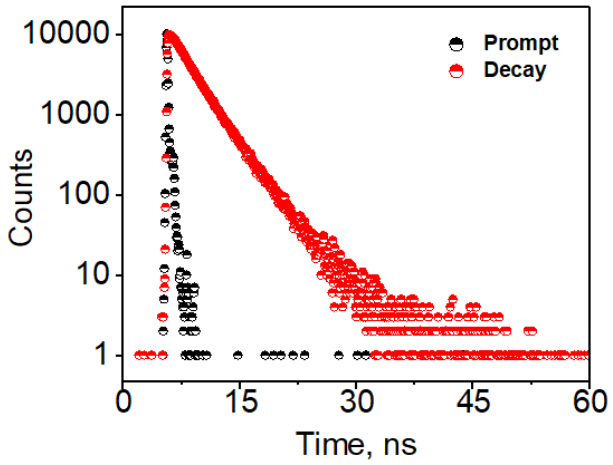

Figure S21: TCSPC ensemble fluorescence decay profile of TDI-TPA$_4$ in HEX.

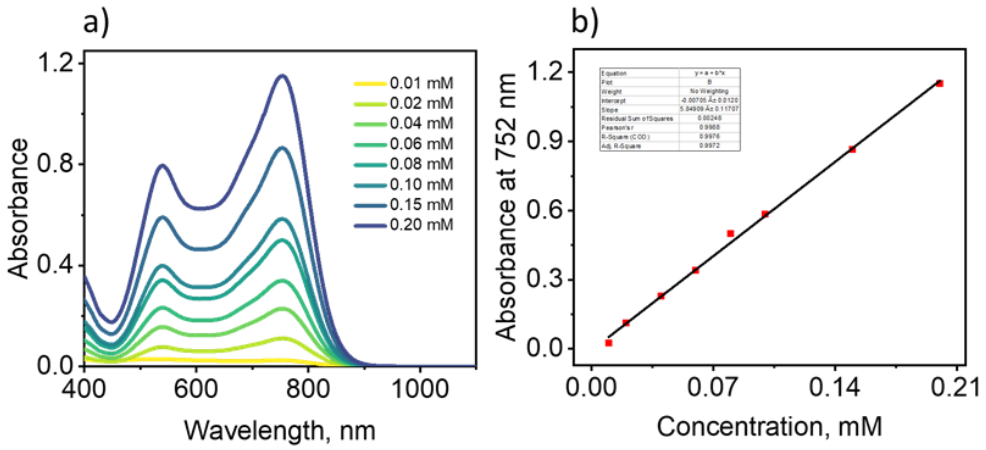

Figure S22: a) Concentration-dependent absorption spectra of TDI-TPA$_4$ in THF and b) Linear plot of absorbance versus concentration (λ=752 nm and path length of the cuvette=2 mm).

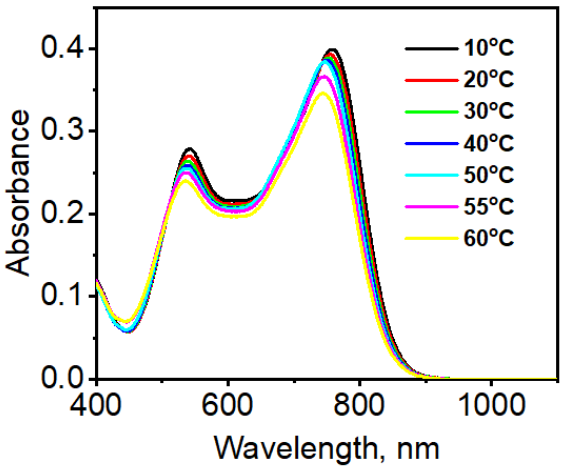

Figure S23: Temperature-dependent absorption spectra of TDI-TPA$_4$ in THF 10°C to 60°C.

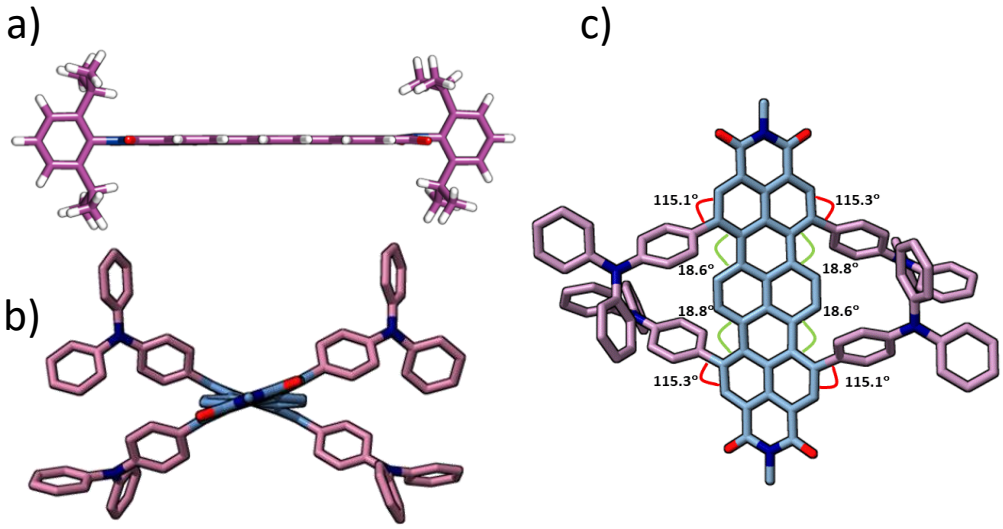

Figure S24: a) Optimized geometry of TDI in the ground state. b) and c) Optimized geometry of TDI-TPA$_4$ in the ground. (2,6-diisopropylphenyl group has been replaced with methyl group to reduce computational cost. Hydrogen atoms are omitted for clarity).

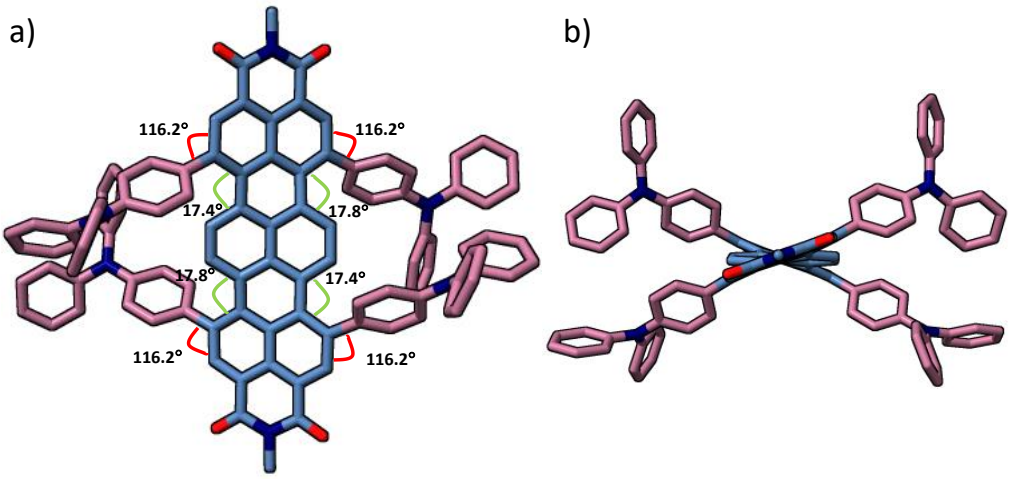

Figure S25: First excited singlet (S_1) optimized geometry of TDI-TPA$_4$ in vacuum**.**

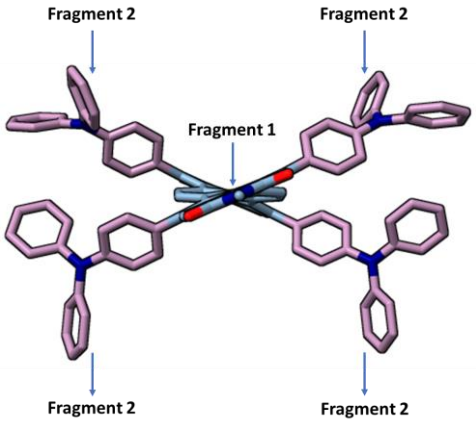

Figure S26: TDI-TPA$_4$ fragmentation used for the TheoDORE analyses.

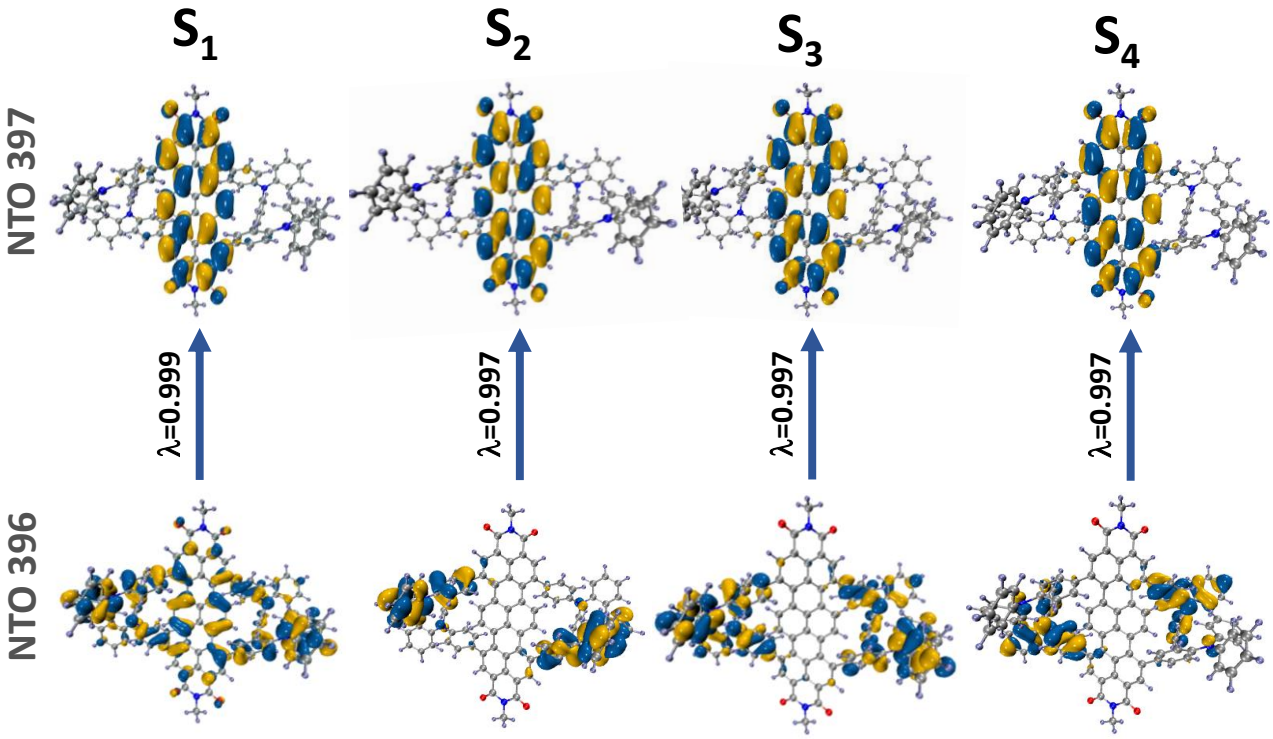

Figure S27: TD-DFT calculated natural transition orbitals (NTO) of the four lowest excited singlet states of TDI-TPA$_4$. The corresponding weightage of NTO (λ) is mentioned (Isovalue=0.02.

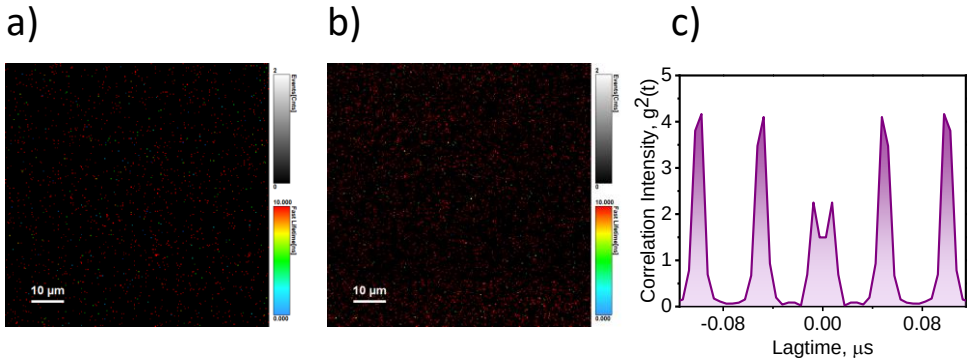

Figure S28: a) FLIM image of a plasma-cleaned cover slip and b) FLIM image of a PS-coated cover slip showing negligible background counts. c) Antibunching data acquired in the PS matrix showing the afterglow doublet peak at zero delay point.

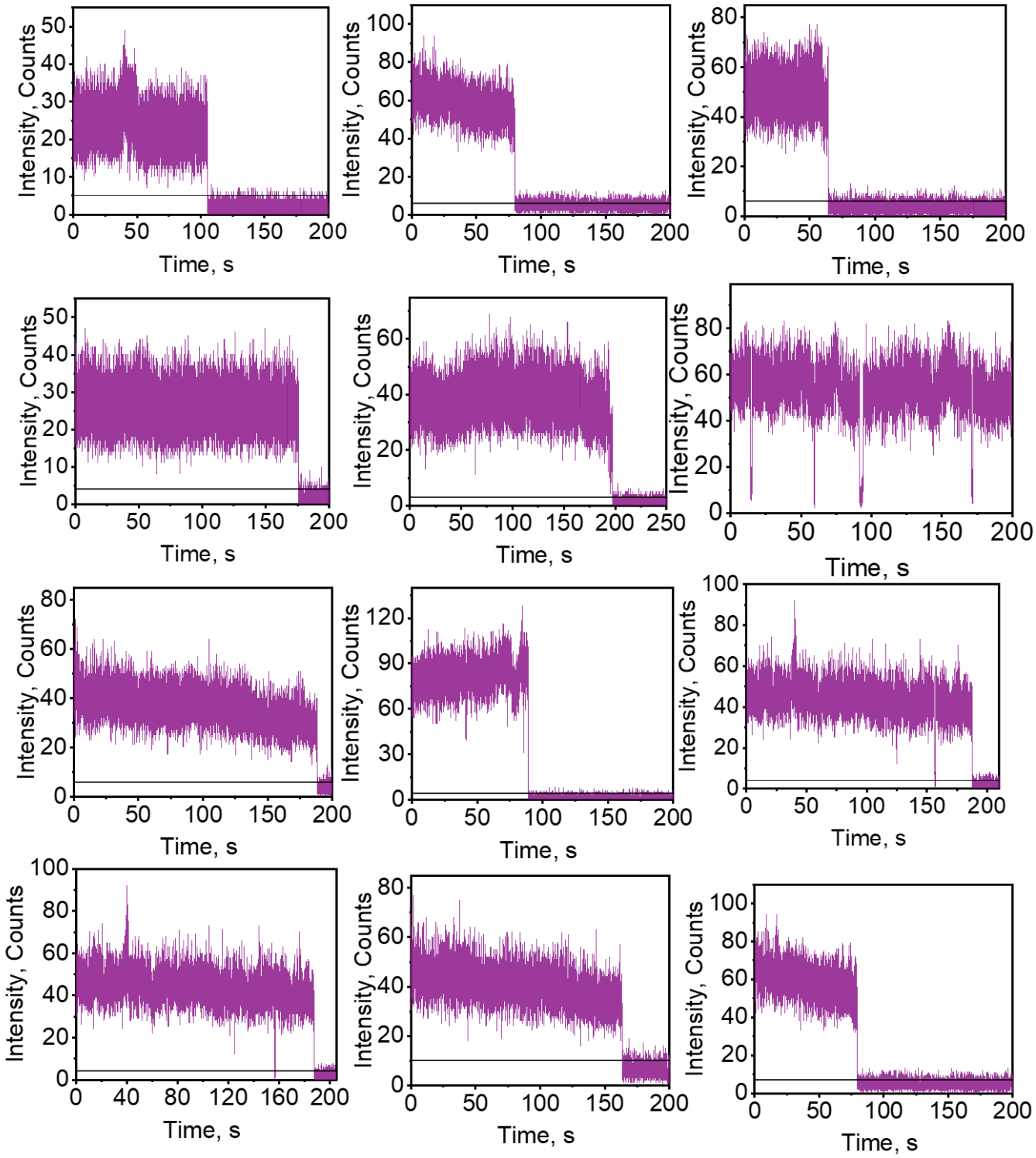

Figure S29: Representative FITs of TDI-TPA$_4$ in polystyrene.

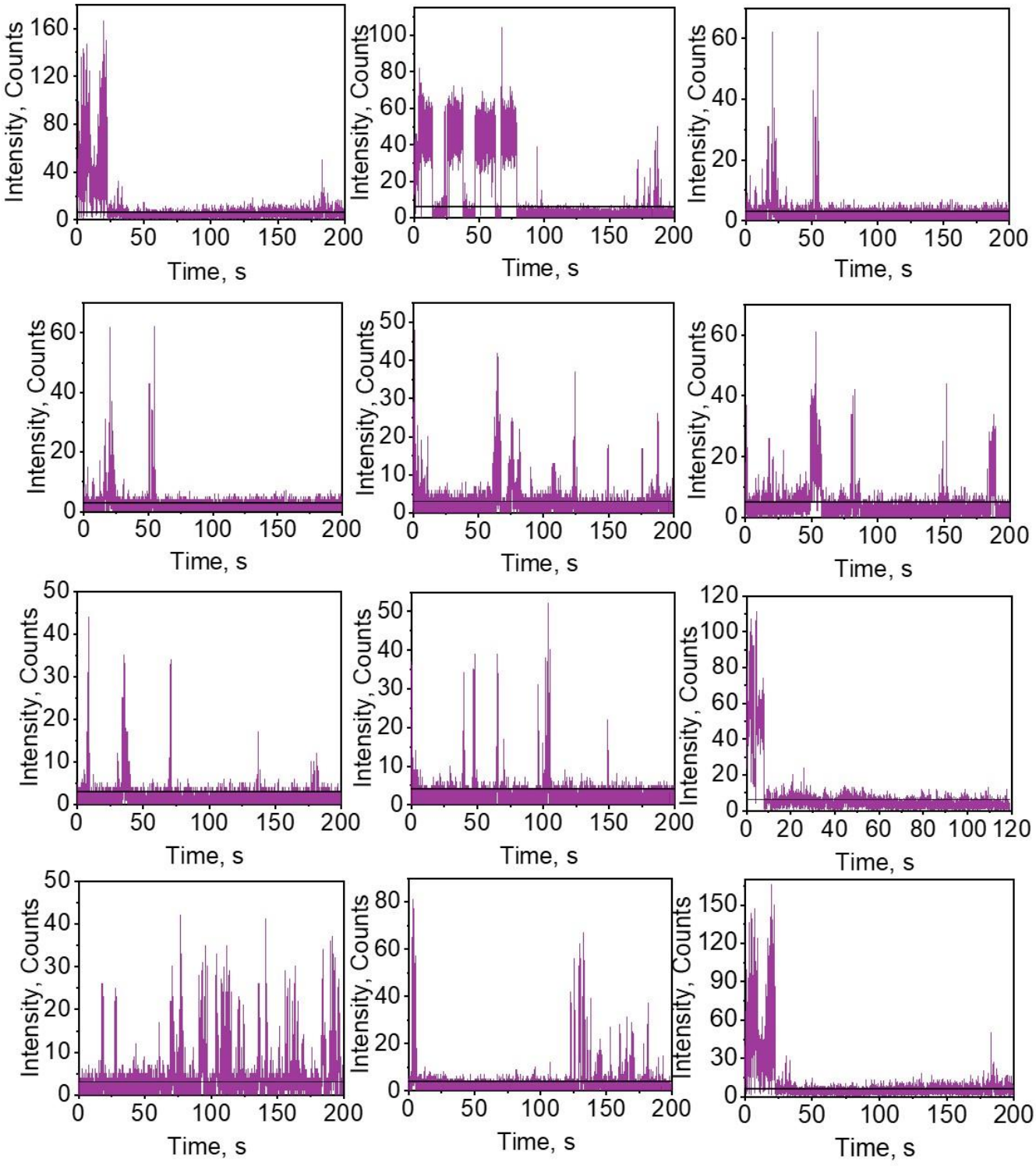

Figure S30: Representative FITs of TDI-TPA$_4$ in poly(vinyl alcohol).

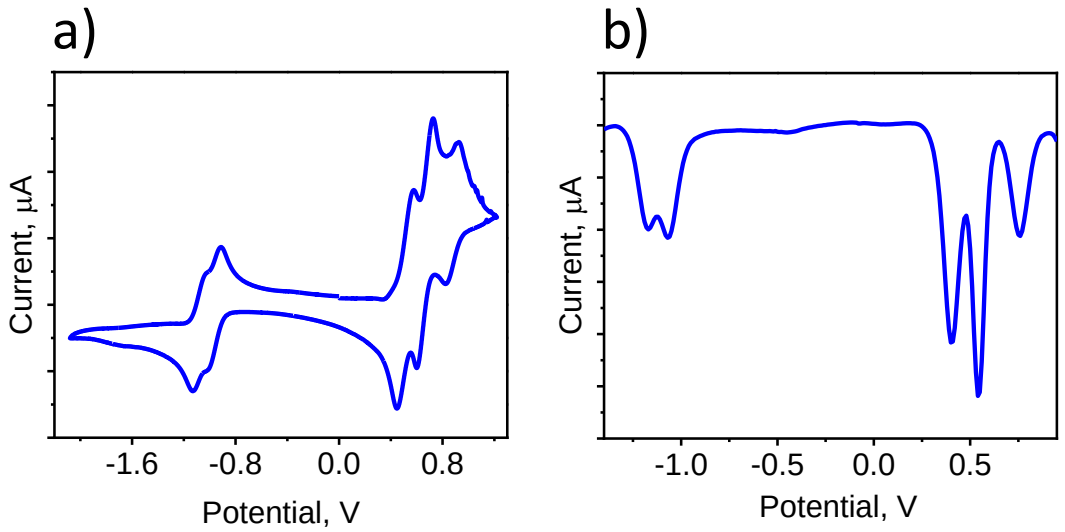

Figure S31: (a) Cyclic voltammetry data and (b) differential pulse voltammogram of TDI-TPA$_4$ in CH_2Cl_2. (Tetrabutylammonium hexafluorophosphate (0.1 M) as the supporting electrolyte, scan rate 200 mV s^{-1}. Fc/Fc^+=ferrocene/ferrocenium couple)

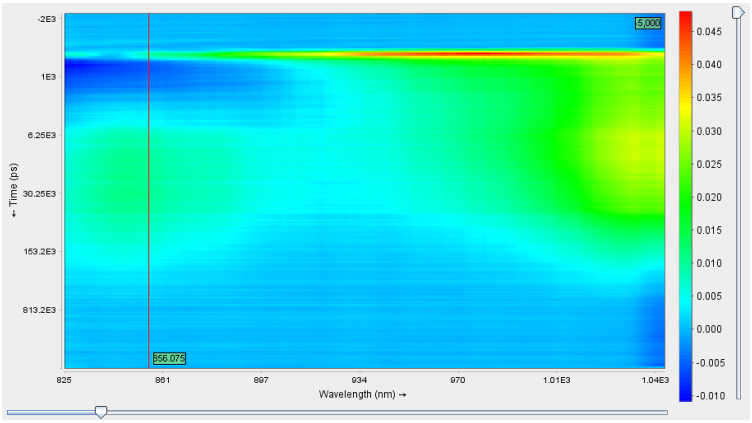

Figure S32: Femtosecond transient absorption contour map recorded in THF showing the evolution of a new species in the wavelength region ~829-906 nm in the later time delay.

Note: The intense signal within 250 fs is a nonlinear solvent response and does not arise from the sample.

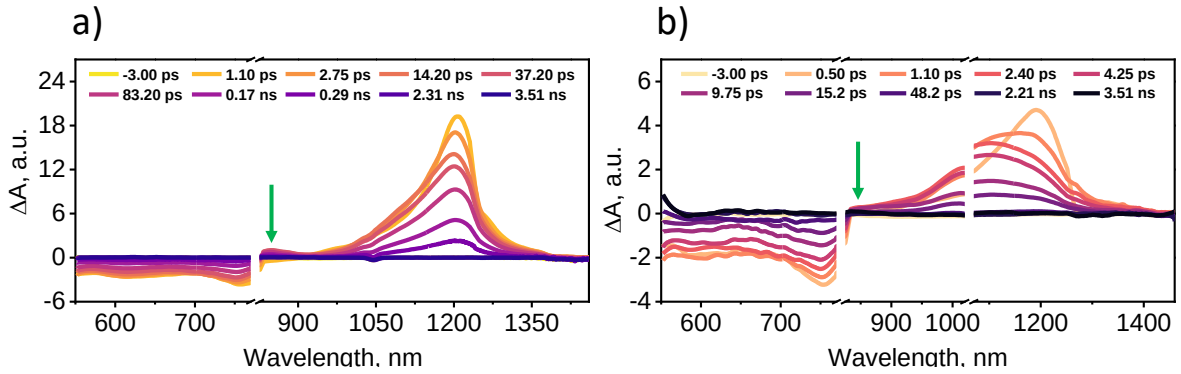

Figure S33: Femtosecond transient absorption spectra of TDI-TPA$_4$ in a) THF and b) ACN showing the evalution radical cation.

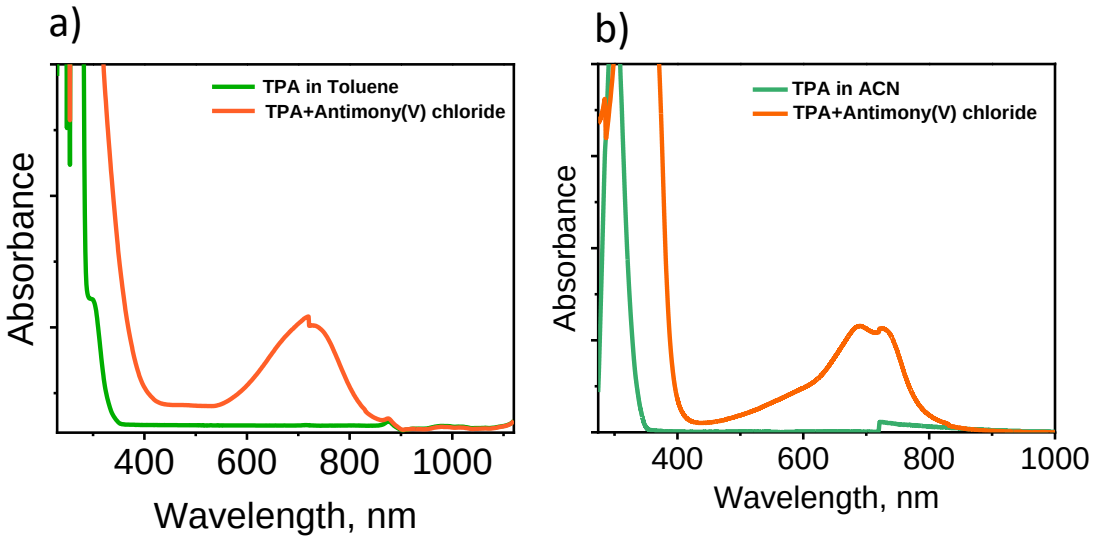

Figure S34: Vis/NIR absorption spectra of TDI-TPA$_4$ in a) toluene and b) ACN with the addition of antimony(V) chloride.

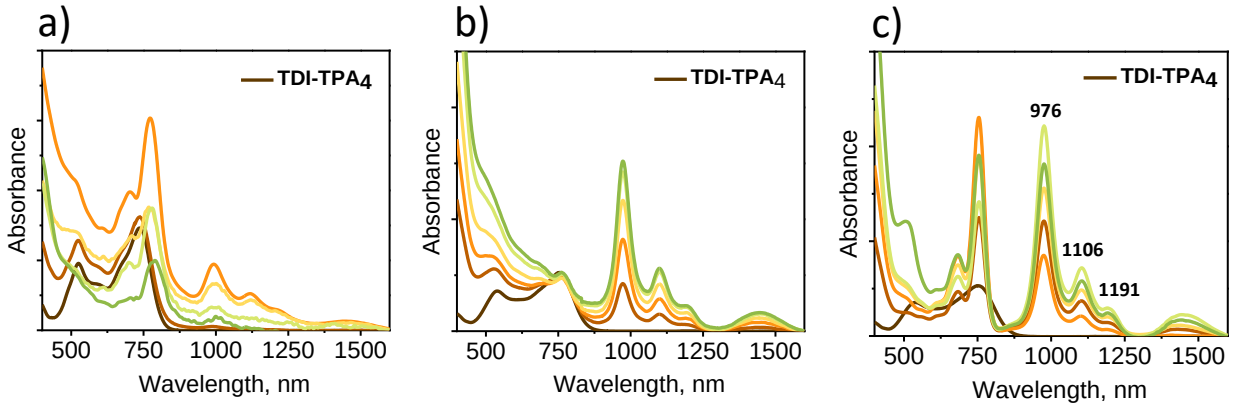

Figure S35: Vis/NIR absorption of TDI-TPA$_4$ in a) HEX, b) THF, and c) ACN recorded upon addition of cobaltocene.

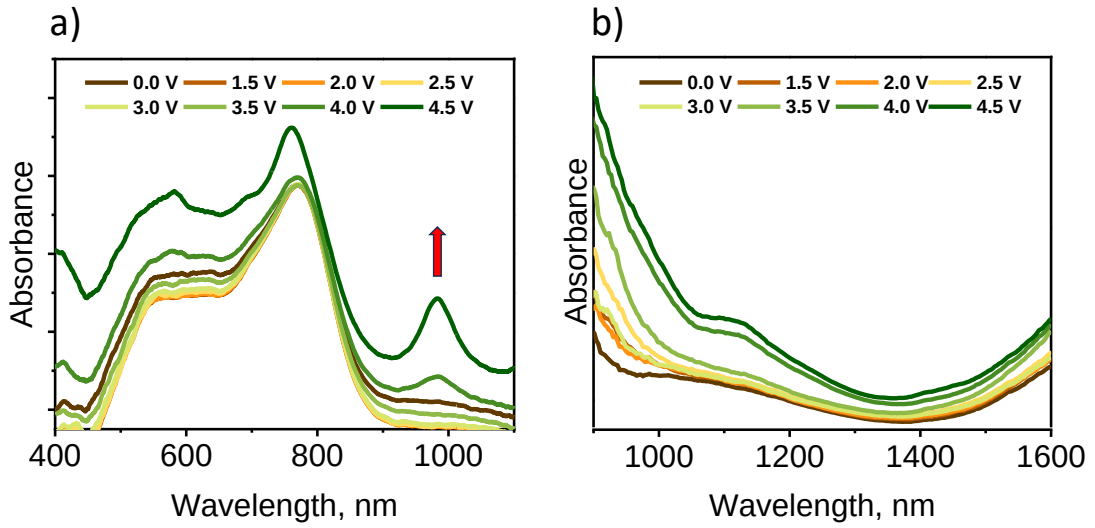

Figure S36: Spectroelectrochemistry measurements of TDI-TPA$_4$ in DCM.

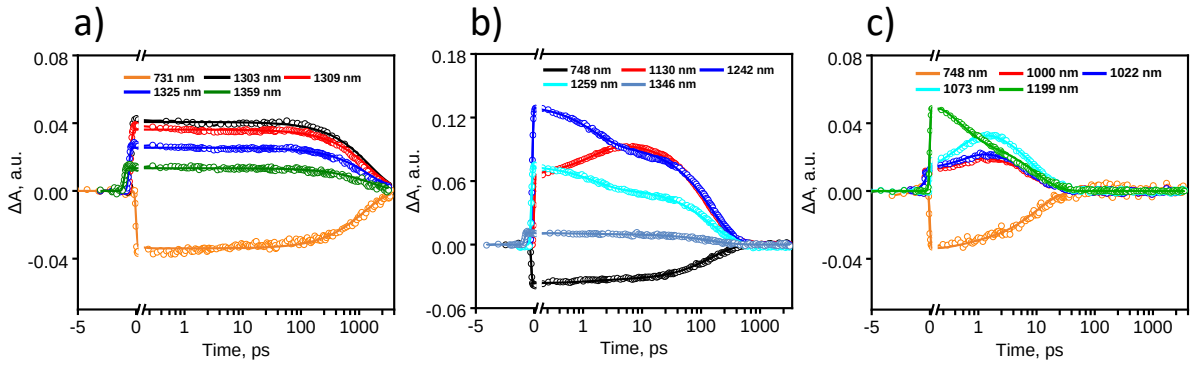

Figure S37: Global analysis fits for selected fsTA wavelengths of TDI-TPA$_4$ (λ_{ex} = 520 nm) in HEX (A→GS) b) THF (A→B→GS) and c) (A→B→GS) kinetic model. Fits are shown as solid lines.

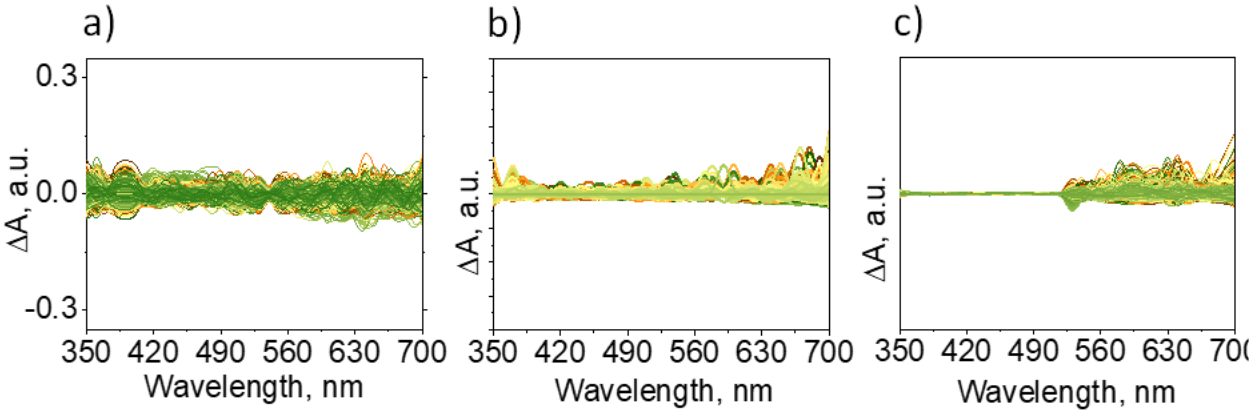

Figure S38: a) Nanosecond transient absorption spectra of TDI-TPA$_4$ in a) HEX, b) THF, and c) ACN.

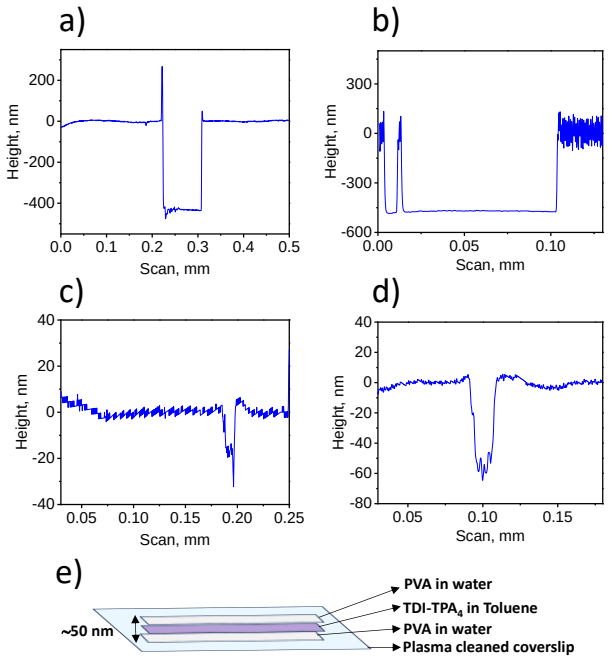

Figure S39: Profilometry traces of TDI-TPA$_4$ thin film used for fsTA measurements in a) PS and b) PVA matrices and for single-molecule fluorescence measurements in c) PS and d) PVA matrices. e) Schematic representation of the single-molecule thin film preparation in PVA matrix.

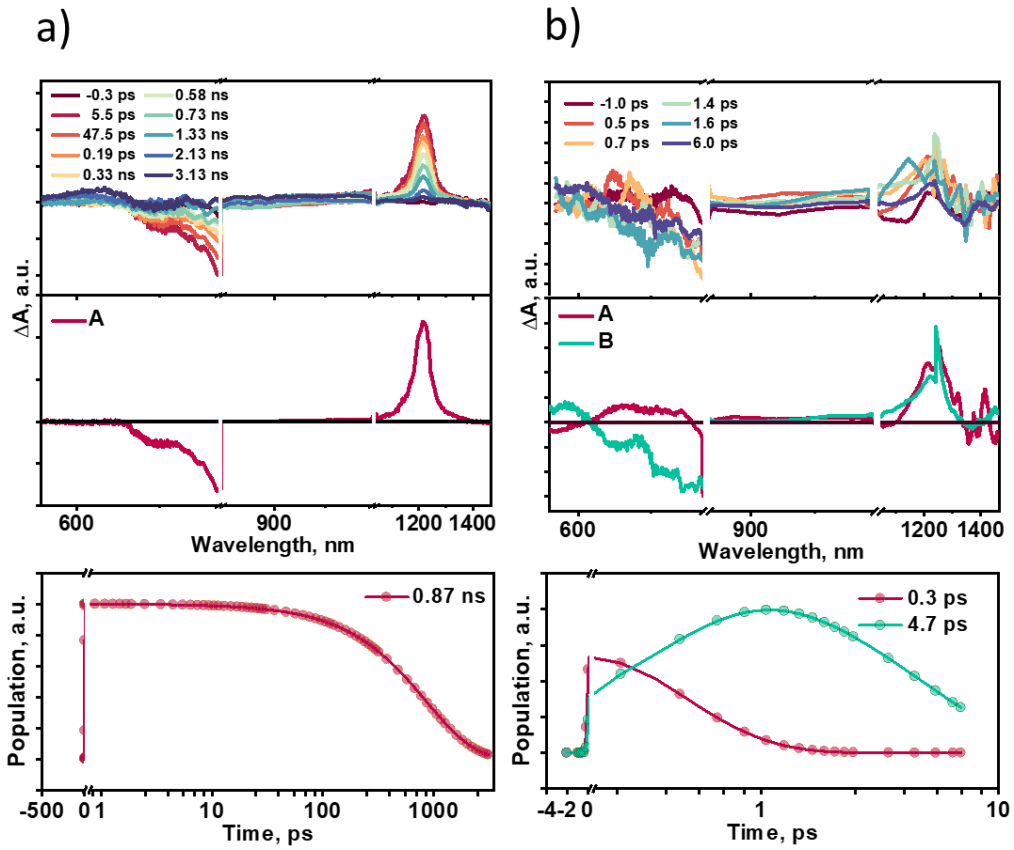

Figure S40: (Top row) Femtosecond transient absorption spectra of TDI-TPA$_4$ in (a) PS, and in (b) PVA matrices (λ_{ex} = 520 nm). (Middle row) Species-associated spectra reconstructed from global analysis of TDI-TPA$_4$ with A → GS model for PS (left), the A → B → GS model for PVA (right). (Bottom row) Relative population profiles of the excited states in TDI-TPA$_4$ in PS and PVA matrices.

Section 4: Coordinates

0 1

C	-1.97866800	5.11340500	1.01244300
C	-2.09712900	3.70834800	0.99159700
C	-1.06146200	2.93044900	0.44449700
C	0.16113700	3.57697300	0.05484700
C	0.22635400	4.99428500	0.06162300
C	-0.86374400	5.75435700	0.53362400
C	1.31911500	2.82481100	-0.34148600
C	2.42073600	3.50832600	-0.88589900
C	2.43151000	4.91871600	-0.89160500
C	1.38188500	5.65618200	-0.40359700
C	-1.16421700	1.47635600	0.20872000
C	0.03161400	0.71392500	0.04809000
C	1.29044400	1.36711100	-0.11128100
C	-2.37069800	0.79718500	0.14340200
C	-2.43208400	-0.58459000	-0.04502400
C	-1.29044400	-1.36712000	-0.11127400
C	-0.03161300	-0.71393600	0.04808700
C	1.16421900	-1.47636600	0.20870300
C	2.37070000	-0.79719800	0.14337100
C	2.43208500	0.58457800	-0.04505000
C	-1.31911400	-2.82481800	-0.34148900
C	-0.16113500	-3.57698000	0.05483300
C	1.06146500	-2.93045900	0.44447800
C	-2.42073600	-3.50833000	-0.88590100
C	-2.43151100	-4.91871900	-0.89161500
C	-1.38188500	-5.65618700	-0.40361500
C	-0.22635100	-4.99429100	0.06160300
C	0.86374900	-5.75436600	0.53359500
C	1.97867500	-5.11341500	1.01241300
C	2.09713300	-3.70835800	0.99157200
C	1.47098600	7.13758100	-0.40993200
N	0.35941100	7.83061800	0.07575500
C	-0.80795500	7.23548900	0.55188200
O	2.45172700	7.72358900	-0.81396800
O	-1.72111900	7.92155300	0.95734900
C	0.39604200	9.28660300	0.09732800
C	-1.47098500	-7.13758700	-0.40995700
N	-0.35940800	-7.83062600	0.07572200
C	0.80796000	-7.23549800	0.55184700
O	-2.45172700	-7.72359300	-0.81399300
O	1.72112600	-7.92156400	0.95730800
C	-0.39603700	-9.28661000	0.09728800
C	4.57543700	1.48088500	-3.26897900
C	3.46929100	2.04795000	-2.65375300
C	3.60446900	2.86279200	-1.52371700
C	4.89649700	3.10806900	-1.04925200
C	6.00952600	2.52640100	-1.64553500
C	5.86726900	1.69830500	-2.76613000
N	6.98817200	1.09782000	-3.37503800
C	6.88255000	-0.20996100	-3.91806700
C	8.22163500	1.78882600	-3.46629400
C	6.28955000	-1.24024800	-3.17999900
C	6.18257100	-2.51785800	-3.71889600
C	6.68071400	-2.79217100	-4.99051500
C	7.28160700	-1.77132000	-5.72322300
C	7.37575100	-0.48695100	-5.19761500
C	9.42768700	1.11447200	-3.23665100
C	10.64055100	1.78790500	-3.33880500
C	10.67328600	3.14414900	-3.65392200
C	9.47560500	3.81893900	-3.87841800
C	8.25955600	3.14912800	-3.79617300
C	-6.62137100	2.53709700	5.58233700
C	-6.75674400	2.42031100	6.96144500
C	-7.31640500	1.27531200	7.52349300
C	-7.73265600	0.24130100	6.68827800
C	-7.58415200	0.34263000	5.30926400
C	-7.02916000	1.49528500	4.74028100
N	-6.88541000	1.60712800	3.33571100
C	-7.92096300	1.15262000	2.48056900
C	-5.70556100	2.14660100	2.78077300
C	-9.25954500	1.44590700	2.76595500
C	-10.27252100	0.99186700	1.92763300
C	-9.96911100	0.25635800	0.78429100
C	-8.63770300	-0.03126600	0.49258900
C	-7.62135000	0.40188000	1.33723500
C	-5.76352300	2.99407200	1.66787900
C	-4.59856500	3.49257500	1.09700700
C	-3.34039700	3.16470700	1.61138900
C	-3.29047100	2.35341300	2.75031000
C	-4.44789400	1.84536300	3.32275000
C	5.76352900	-2.99408500	1.66784900
C	4.59856900	-3.49258800	1.09698000

C	3.34040300	-3.16471700	1.61136100
C	3.29047800	-2.35342100	2.75028000
C	4.44790200	-1.84537100	3.32271800
C	5.70556800	-2.14661100	2.78074200
N	6.88541900	-1.60713800	3.33567800
C	7.02917000	-1.49529100	4.74024700
C	7.92097100	-1.15263200	2.48053300
C	6.62137900	-2.53710000	5.58230600
C	6.75675200	-2.42031000	6.96141400
C	7.31641700	-1.27531100	7.52345900
C	7.73267000	-0.24130400	6.68824000
C	7.58416500	-0.34263700	5.30922700
C	9.25955300	-1.44591700	2.76591800
C	10.27252800	-0.99187800	1.92759400
C	9.96911600	-0.25637400	0.78425000
C	8.63770700	0.03124800	0.49254800
C	7.62135500	-0.40189600	1.33719600
C	-6.28956200	1.24026200	-3.17993200
C	-6.18258800	2.51788100	-3.71880800
C	-6.68073800	2.79221400	-4.99042000
C	-7.28163300	1.77137400	-5.72314200
C	-7.37577200	0.48699700	-5.19755500
C	-6.88256400	0.20998700	-3.91801300
N	-6.98818100	-1.09780400	-3.37500500
C	-8.22164400	-1.78881100	-3.46626800
C	-5.86727600	-1.69829400	-2.76610700
C	-9.42769700	-1.11446300	-3.23661200
C	-10.64055900	-1.78789800	-3.33877200
C	-10.67329200	-3.14413800	-3.65390800
C	-9.47560900	-3.81892200	-3.87841600
C	-8.25956200	-3.14910900	-3.79616500
C	-4.57544500	-1.48086600	-3.26895500
C	-3.46929800	-2.04793700	-2.65373800
C	-3.60447200	-2.86279100	-1.52371100
C	-4.89649900	-3.10807600	-1.04924700
C	-6.00953000	-2.52640400	-1.64552100
H	-2.78858200	5.71968700	1.42065500
H	3.29241900	5.45197700	-1.29690700
H	-3.30891300	1.33628500	0.21686400
H	-3.41424100	-1.04005000	-0.11580300
H	3.30891500	-1.33629900	0.21682000
H	3.41424200	1.04003800	-0.11583900
H	-3.29242100	-5.45197700	-1.29691700
H	2.78859100	-5.71969700	1.42062000
H	1.36233200	9.60462700	-0.30316600
H	-0.42427900	9.69362200	-0.50898800
H	0.26603200	9.65200100	1.12485200
H	-1.36232900	-9.60463300	-0.30320300
H	-0.26602300	-9.65201300	1.12481100
H	0.42428100	-9.69362600	-0.50903300
H	4.44290800	0.85881200	-4.15482800
H	2.47468200	1.85816200	-3.06279500
H	5.03591600	3.74390600	-0.17195000
H	7.00251700	2.71911100	-1.23765900
H	5.91236700	-1.03303900	-2.17725700
H	5.71562900	-3.31121200	-3.13109000
H	6.60178800	-3.79768900	-5.40814500
H	7.67248200	-1.97229100	-6.72310300
H	7.83699700	0.31390800	-5.77771300
H	9.40840900	0.05408500	-2.98033000
H	11.57136600	1.24488700	-3.15991900
H	11.62619800	3.67158700	-3.72667100
H	9.48536900	4.88050200	-4.13531600
H	7.32683100	3.68147900	-3.98796200
H	-6.19587000	3.44278400	5.14744400
H	-6.43216600	3.24259900	7.60299100
H	-7.42815800	1.18969300	8.60600300
H	-8.16867200	-0.66483500	7.11479500
H	-7.90094900	-0.47569100	4.66107100
H	-9.50126200	2.03297700	3.65328900
H	-11.31174900	1.22858000	2.16658100
H	-10.76392400	-0.09404900	0.12306900
H	-8.38664400	-0.60934100	-0.39917100
H	-6.58194600	0.15793100	1.11226000
H	-6.73343200	3.25752000	1.24414300
H	-4.66918900	4.14424400	0.22290000
H	-2.32162500	2.09213600	3.18118200
H	-4.38195400	1.19978500	4.19943100
H	6.73343700	-3.25753600	1.24411400
H	4.66919200	-4.14425800	0.22287400
H	2.32163200	-2.09214200	3.18115200
H	4.38196300	-1.19979100	4.19939900
H	6.19587400	-3.44278700	5.14741700
H	6.43217200	-3.24259500	7.60296300
H	7.42817000	-1.18968900	8.60596800

H	8.16868900	0.66483200	7.11475500
H	7.90096400	0.47568200	4.66103100
H	9.50127200	-2.03298400	3.65325400
H	11.31175700	-1.22859000	2.16654100
H	10.76392800	0.09403200	0.12302500
H	8.38664700	0.60932000	-0.39921300
H	6.58195100	-0.15794900	1.11222100
H	-5.91237400	1.03303700	-2.17719500
H	-5.71564400	3.31122600	-3.13099100
H	-6.60181600	3.79773900	-5.40803400
H	-7.67251400	1.97236100	-6.72301700
H	-7.83702000	-0.31385400	-5.77766300
H	-9.40842100	-0.05408000	-2.98027600
H	-11.57137500	-1.24488500	-3.15987600
H	-11.62620300	-3.67157700	-3.72666100
H	-9.48537100	-4.88048200	-4.13532900
H	-7.32683700	-3.68145500	-3.98796300
H	-4.44291900	-0.85878300	-4.15479700
H	-2.47469000	-1.85814200	-3.06277800
H	-5.03591400	-3.74392300	-0.17195100
H	-7.00252000	-2.71912100	-1.23764600

Section 5: References

1. J. R. Lakowicz, *Principles of Fluorescence Spectroscopy*, Springer, Berlin, 3rd Edition edn., 2006.
2. C. Erker and T. Basché, The Energy Gap Law at Work: Emission Yield and Rate Fluctuations of Single NIR Emitters, *J. Am. Chem. Soc.*, 2022, **144**, 14053-14056.
3. G. W. T. M. J. Frisch, H. B. Schlegel, G. E. Scuseria, M. A. Robb, J. R. Cheeseman, G. Scalmani, V. Barone, G. A. Petersson, H. Nakatsuji, X. Li, M. Caricato, A. V. Marenich, J. Bloino, B. G. Janesko, R. Gomperts, B. Mennucci, H. P. Hratchian, J. V. Ortiz, A. F. Izmaylov, J. L. Sonnenberg, D. Williams-Young, F. Ding, F. Lipparini, F. Egidi, J. Goings, B. Peng, A. Petrone, T. Henderson, D. Ranasinghe, V. G. Zakrzewski, J. Gao, N. Rega, G. Zheng, W. Liang, M. Hada, M. Ehara, K. Toyota, R. Fukuda, J. Hasegawa, M. Ishida, T. Nakajima, Y. Honda, O. Kitao, H. Nakai, T. Vreven, K. Throssell, J. A. Montgomery Jr., J. E. Peralta, F. Ogliaro, M. J. Bearpark, J. J. Heyd, E. N. Brothers, K. N. Kudin, V. N. Staroverov, T. A. Keith, R. Kobayashi, J. Normand, K. Raghavachari, A. P. Rendell, J. C. Burant, S. S. Iyengar, J. Tomasi, M. Cossi, J. M. Millam, M. Klene, C. Adamo, R. Cammi, J. W. Ochterski, R. L. Martin, K. Morokuma, O. Farkas, J. B. Foresman, D. J. Fox,, in Gaussian 16, 2016, Gaussian, Inc., Vol. Revision C.01, Wallingford CT.
4. T. Lu and F. Chen, Multiwfn: A multifunctional wavefunction analyzer, *J. Comput. Chem.*, 2012, **33**, 580-592.
5. F. Plasser, TheoDORE: A toolbox for a detailed and automated analysis of electronic excited state computations, *J. Chem. Phys.*, 2020, **152**, 084108.
6. F. Plasser and H. Lischka, Analysis of Excitonic and Charge Transfer Interactions from Quantum Chemical Calculations, *J. Chem. Theory Comput.*, 2012, **8**, 2777-2789.
7. Y.-L. Wu, K. E. Brown and M. R. Wasielewski, Extending Photoinduced Charge Separation Lifetimes by Using Supramolecular Design: Guanine–Perylenediimide G-Quadruplex, *J. Am. Chem. Soc.*, 2013, **135**, 13322-13325.
8. K. N. Prajapati, B. Johns, K. Bandopadhyay, S. R. P. Silva and J. Mitra, Interaction of ZnO nanorods with plasmonic metal nanoparticles and semiconductor quantum dots, *J. Chem. Phys.*, 2020, **152**, 064704.
9. A. Weller, Photoinduced Electron Transfer in Solution: Exciplex and Radical Ion Pair Formation Free Enthalpies and their Solvent Dependence, 1982, **133**, 93-98.
10. P. Deng, L. Liu, S. Ren, H. Li and Q. Zhang, N-acylation: an effective method for reducing the LUMO energy levels of conjugated polymers containing five-membered lactam units, *Chem. Commun.*, 2012, **48**, 6960-6962.
11. J. J. Snellenburg, S. Laptenok, R. Seger, K. M. Mullen and I. H. M. van Stokkum, Glotaran: A Java-Based Graphical User Interface for the R Package TIMP, *J. Stat. Softw.*, 2012, **49**, 1 - 22.
12. M. W. Holman, R. Liu and D. M. Adams, Single-Molecule Spectroscopy of Interfacial Electron Transfer, *J. Am. Chem. Soc.*, 2003, **125**, 12649-12654.